Submitted to *International Journal of Robotics and Automation*, July 2003.

THE REACH ENVELOPE OF A 9 DEGREE-OF-FREEDOM MODEL OF THE UPPER EXTREMITY

by

Jingzhou Yang*[1] , Karim Abdel-Malek[1] , and Kyle Nebel[2]
[1]Digital Humans Laboratory
Center for Computer-Aided Design
The University of Iowa
242 Engineering Research Facilities
Iowa City, IA 52242-1000
Tel No: (319) 335-6053
Fax No: (319) 384-0542

[2]U.S. Army TACOM
MAIL STOP #233
National Automotive Center
6501 East 11 Mile Rd.
Warren, MI 48397-5000
Tel: (586) 574-8809

E-mail: **jyang@engineering.uiowa.edu**

Original Submission: July 2003
* Author to whom all correspondence should be addressed

Report Documentation Page

Form Approved
OMB No. 0704-0188

1. REPORT DATE	2. REPORT TYPE	3. DATES COVERED
01 JUL 2003	**Technical Report**	**01-07-2003 to 01-07-2003**

4. TITLE AND SUBTITLE
The Reach Envelope of a 9 Degree-of-Freedom model of the upper extremity

5a. CONTRACT NUMBER
5b. GRANT NUMBER
5c. PROGRAM ELEMENT NUMBER

6. AUTHOR(S)
jingzhou Yang; Karim Malek-Abdel; Kyle Nebel

5d. PROJECT NUMBER
5e. TASK NUMBER
5f. WORK UNIT NUMBER

7. PERFORMING ORGANIZATION NAME(S) AND ADDRESS(ES)
Digital Humans Laboratory,Center for Computer-Aided Deisgn University of Iowa, 242 Engineering Research Facilities ,Iowa City,IA,52242-1000

8. PERFORMING ORGANIZATION REPORT NUMBER
; #13980

9. SPONSORING/MONITORING AGENCY NAME(S) AND ADDRESS(ES)
U.S. Army TARDEC, 6501 E.11 Mile Rd, Warren, MI, 48397-5000

10. SPONSOR/MONITOR'S ACRONYM(S)

11. SPONSOR/MONITOR'S REPORT NUMBER(S)
#13980

12. DISTRIBUTION/AVAILABILITY STATEMENT
Approved for public release; distribution unlimited

13. SUPPLEMENTARY NOTES

14. ABSTRACT

This paper presents a rigorous mathematical formulation for modeling the upper extremity that is capable of considering a relatively large number of degrees of freedom, thus yielding a realistic model and associated envelope. Kinematic models are used to determine the reach envelope in closed-form and to better understand human motion. Joint ranges of motion are taken into account by transforming unilateral inequality constraints into equalities that are included in the formulation. Methods from geometry are implemented to analyze the motion and delineate barriers within the workspace. It is observed that these barriers are indeed surfaces where the limb has one or more joints at their limits, but also where the hand?s motion has encountered a kinematic singular configuration. Such a configuration is mathematically defined and is physically associated with two links being parallel at an instant in time or where two joints have their axes parallel (e.g., a fully extended arm yields a singular configuration). Barriers to motion can now be characterized in terms of different human performance measures, thus leading to a better understanding of the path trajectories assumed by humans as they execute tasks.

15. SUBJECT TERMS
Keywords: Reach envelope, ergonomics, shoulder complex, elbow, wrist.

16. SECURITY CLASSIFICATION OF:			17. LIMITATION OF ABSTRACT	18. NUMBER OF PAGES	19a. NAME OF RESPONSIBLE PERSON
a. REPORT	b. ABSTRACT	c. THIS PAGE			
unclassified	**unclassified**	**unclassified**	**Same as Report (SAR)**	**39**	

Abstract

This paper presents a rigorous mathematical formulation for modeling the upper extremity that is capable of considering a relatively large number of degrees of freedom, thus yielding a realistic model and associated envelope. Kinematic models are used to determine the reach envelope in closed-form and to better understand human motion. Joint ranges of motion are taken into account by transforming unilateral inequality constraints into equalities that are included in the formulation. Methods from geometry are implemented to analyze the motion and delineate barriers within the workspace. It is observed that these barriers are indeed surfaces where the limb has one or more joints at their limits, but also where the hand's motion has encountered a kinematic singular configuration. Such a configuration is mathematically defined and is physically associated with two links being parallel at an instant in time or where two joints have their axes parallel (e.g., a fully extended arm yields a singular configuration). Barriers to motion can now be characterized in terms of different human performance measures, thus leading to a better understanding of the path trajectories assumed by humans as they execute tasks.

Keywords: Reach envelope, ergonomics, shoulder complex, elbow, wrist.

1. Introduction

Analytical methods in the field of robotics have significantly contributed to the evaluation, programming, and design of mechanical robotic manipulators and similar devices. The motivation for investigating the motion of human limbs using such mathematical methods is twofold: to achieve a better understanding of functionality, in terms of evaluative measures, and to obtain more rigorous methods for designing ergonomic workspaces. The ultimate goal of this research, however, is to develop a method for identifying injured joints from a path trajectory..

Biomechanical models of the shoulder have been proposed by many researchers, such as qualitative planar kinematic models (Dvir and Berme 1978; Jackson, et al. 1977), but were confined to a single motion pattern. A complex model of the shoulder was proposed by Högfors, *et al*. (1991), in which it was treated as a three-rigid body twelve degree-of-freedom (DOF) system. From a biomechanical point of view, the human arm mechanism, particularly the shoulder joints, are probably the most complex of the human body. The upper extremity is typically modeled as a series of segmental links connected in a special arrangement of one DOF revolute or prismatic joint (Wood et al. 1989, Benati et al. 1980 and Engin et al. 1990). These links have typically been limited to a small number of DOFs because of the difficulty in addressing larger numbers. We will follow a similar modeling method, but will not limit the number of DOFs. Instead, we will develop and demonstrate a mathematical method for analyzing human motion, visualizing the resulting workspace to better understand the barriers therein. Most importantly, we will account for ranges of motion in determining and visualizing the envelope.

In an earlier investigation (Lenarcic et al. 1994), a simple model of a human arm only considers the shoulder complex and the elbow joint where the two translational motions were replaced with two rotational DOFs to simplify the analysis. The European Esprit Project CHARM (Maurel 1998) developed a comprehensive human animation resource model allowing the dynamic simulation of complex musculoskeletal systems, including finite element deformation of soft-tissues and muscular contraction. A biomechanical

model of the human arm and shoulder was designed including properties for bones, joints, and muscle lines of action. However, reach envelopes were not determined. Indeed, many researchers (including commercial human modeling software developers) have adapted a simplified approach of moving the arm through its ranges (arm fully extended) to determine the outer most boundary. While this method yields only one barrier, it is approximate in nature, does not determine all barriers, and does not yield closed form equations of the boundary surfaces.

This paper extends our previous work (Abdel-Malek & Yang 2001) by presenting a practical model of the human arm that includes the resulting motion of the shoulder complex. The first section of this paper reviews the modeling approach and provides a brief anatomy of the upper extremity. In the second section, we present the kinematic model and the theory of swept volumes that we will use to determine the reach envelope. Based on this approach, we use two steps to analyze the human arm workspace. First, we will directly address the workspace of the 7DOFs without the translational motion of the scapulathorasic joint. Second, we will subject the resulting geometry to a sweep motion due to the shoulder translational joints. We are then able to visualize the reach envelope, characterize boundary surfaces in closed form, and describe barriers therein that are due to joint limits.

2. Background

In order to develop a realistic kinematic model of the upper extremity, it is important to understand human anatomy. The upper limb is composed of three chained mechanisms: the shoulder girdle, the elbow and the wrist. If we consider bones in pairs, seven joints may be distinguished: the sterno-clavicular joint, which articulates the clavicle by its proximal end onto the sternum, the acromio-clavicular joint, which articulates the scapula by its acromion onto the distal end of the clavicle, the scapulo-thoracic joint, which allows the scapula to glide on the thorax, the gleno-humeral joint, which allows the humeral head to rotate in the glenoid fossa of the scapula, the ulno-humeral and the humero-radial joints, which articulate both ulna and radius on the distal end of the

humerus, and finally, the ulno-radial joint where both distal ends of ulna and radius join together.

The shoulder girdle is perhaps the most difficult to model because of the extension of some muscles over more than two segmental links and joints. The two main bones of the shoulder are the humerus and the scapula (shoulder blade). The end of the scapula, called the glenoid, meets the head of the humerus to form a glenohumeral cavity that acts as a flexible ball-and-socket joint (Figure 1).

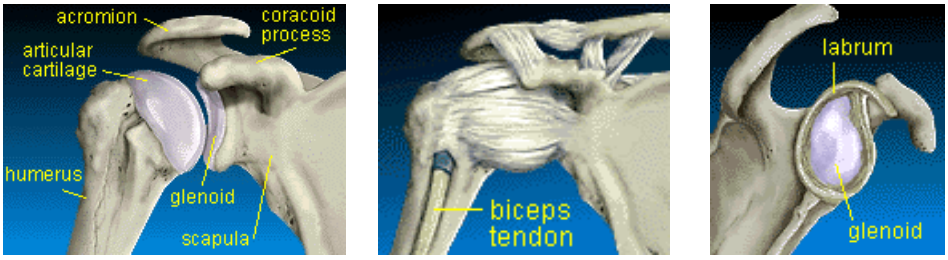

Figure 1. Anatomy of the shoulder complex

Shoulder movements are usually referred to as ventral/dorsal, cranial/caudal and axial rotations for the sterno-clavicular (3 DOFs), as abduction/adduction, flexion/extension and axial rotation for the gleno-humeral joint (3 DOFs), as elevation/depression, protraction/retraction, tipping forward/backward and medial/lateral rotations for the scapulo-thoracic joint (5 DOFs), and as flexion/extension and pronation/supination movements for the forearm joints (2 DOFs). In our modeling, we shall use 5DOFs for the shoulder complex, where we have accounted for 3 rotational and two translational motions (Figure 2).

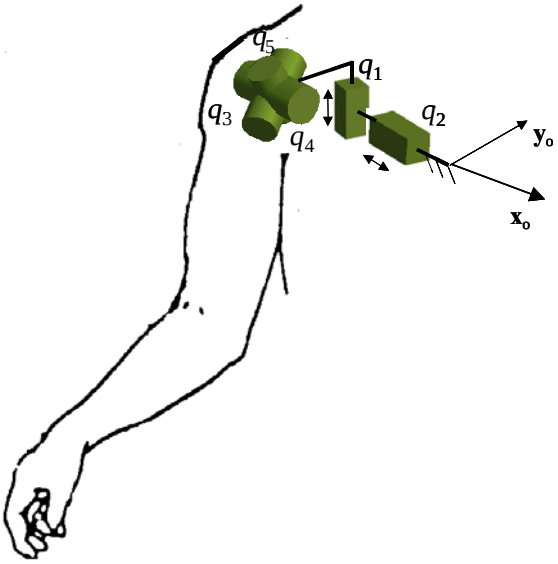

Figure 2. Modeling of the shoulder complex as three revolute and two sliding DOFs

This model allows for consideration of the coupling between some of the joints, as is the case in the shoulder where muscles extend over more than one segment. When muscles are used to lift the arm in a rotational motion a translational motion of the shoulder unwittingly occurs.

The elbow is a hinge joint made up of the humerus, ulna and radius. The unique positioning and interaction of the bones in the joint allows for a small amount of rotation and hinge action. Theprimary stability of the elbow is provided by the ulnar collateral ligament, on the medial (inner) side of the elbow. It is safe to model the elbow as a 1DOF revolute joint.

The hand is composed of many small bones called carpals, metacarpals, and phalanges. The two bones of the lower arm -- the radius and the ulna -- meet at the hand to form the wrist. We will model the wrist as three revolute joints intersecting at one point, whose action yields a spherical wrist (Pieper 1968). The complete 9 DOF model of the upper extremity is shown in Figure 3.

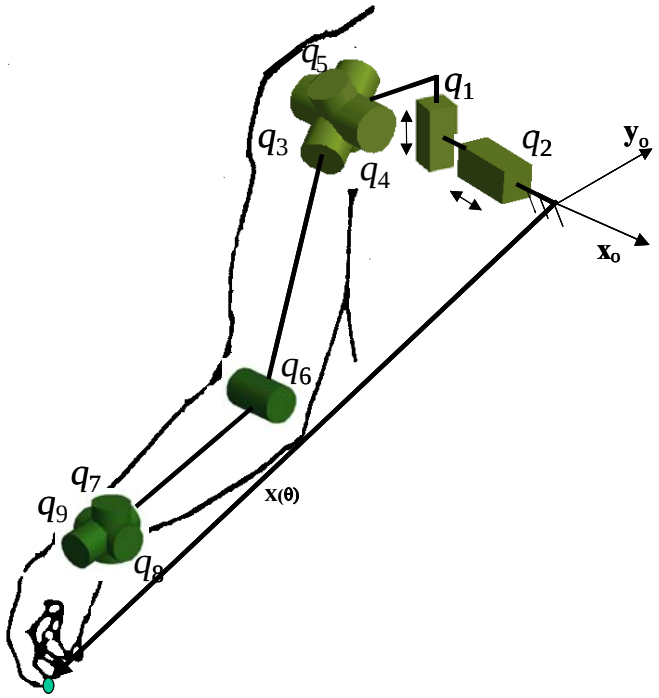

Figure 3. Modeling of the upper extremity as a 9 degree of freedom kinematic chain

Given the respective material properties, bones may be regarded as rigid bodies in contrast to soft tissues with respect to the relevant physiological ranges of motion and force handling. This allows for a rigid body segmental representation of the kinematics among the skeletal subsystem from the soft tissues by converting their relations with the bones into external actions. Therefore, the kinematic model can only be analyzed by considering the skeletal components.

3. Mathematical Formulation

Although the anatomy of the human upper extremity and joints are very complex as evidenced by the debate in the literature on the correct method for modeling joint motion (Engin 1984; Choi 1993; Engin 1989a,b; Hogfors 1991; Raikova 1992; Helm 1994, Maurel 1998), we will employ a kinematic pair (or combination thereof) used in the field of robotics. In fact, all anatomical joints can be modeled using a combination of basic kinematic pairs. Consider the two segmental links connected by a joint in Figure 4. We will use a coordinate frame for each degree of freedom in the system. Because the

shoulder in our model has 5DOFs, for example, it will have five variables associated with it in which each variable is denoted by q_i

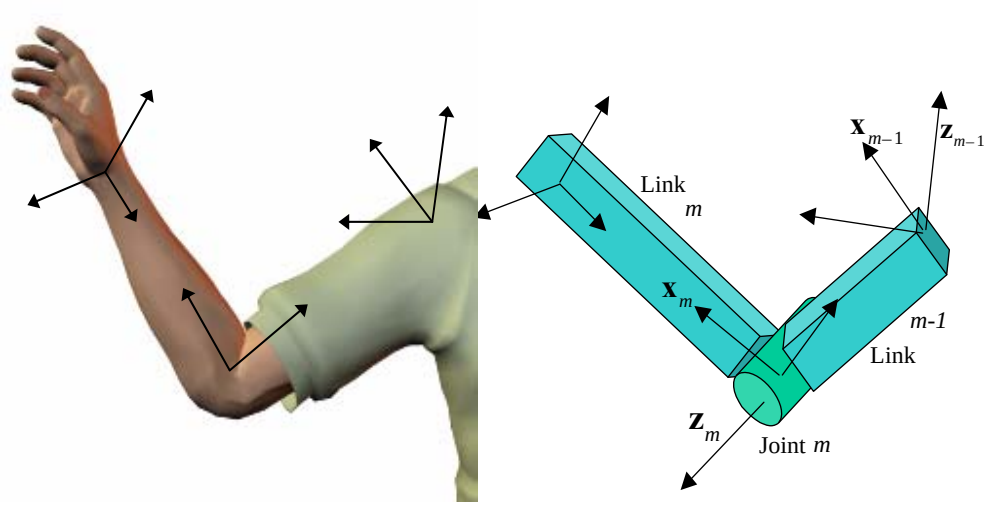

Figure 4. Definition of a kinematic pair (e.g., a revolute joint)

We define $\mathbf{q}^* = [q_1 \ \ldots \ q_n]^T \in \mathbf{R}^n$ as the vector of n-generalized coordinates characterizing the motion of a limb, where q_i (i =1, 2, … , n) represents a DOF. For instance, the elbow joint will be represented by one DOF, for example q_6 (Figure 4), while the wrist joint will be represented by three DOF, namely q_7, q_8 and q_9. The vector function generated by a point of interest written as a multiplication of rotation matrices and position vectors is expressed by

$$\mathbf{\Phi}(\mathbf{q}^*) = \begin{bmatrix} x(\mathbf{q}^*) \\ y(\mathbf{q}^*) \\ z(\mathbf{q}^*) \end{bmatrix} = \sum_{i=1}^{i=n} [\prod_{j=1}^{j=i-1} {}^{j-1}\mathbf{R}_j]\, {}^{i-1}\mathbf{p}_i \tag{1}$$

where both ${}^{i-1}\mathbf{p}_i$ and ${}^{j-1}\mathbf{R}_j$ are defined using the Denavit-Hartenberg (DH) representation method (Denavit and Hartenberg 1955), such that

$${}^{i-1}\mathbf{R}_i = \begin{bmatrix} \cos\theta_i & -\cos\alpha_i \sin\theta_i & \sin\alpha_i \sin\theta_i \\ \sin\theta_i & \cos\alpha_i \cos\theta_i & -\sin\alpha_i \cos\theta_i \\ 0 & \sin\alpha_i & \cos\alpha_i \end{bmatrix} \tag{2}$$

and

$${}^{(i-1)}\mathbf{p}_i = \begin{bmatrix} a_i \cos\theta_i & a_i \sin\theta_i & d_i \end{bmatrix}^T \tag{3}$$

where θ_i is the joint angle from the $\mathbf{x}_{i-1}$ axis to the $\mathbf{x}_i$ axis, d_i is the shortest distance between $\mathbf{x}_{i-1}$ and $\mathbf{x}_i$ axes, a_i is the offset distance between $\mathbf{z}_i$ and $\mathbf{z}_{i-1}$ axes, and α_i is the offset angle from $\mathbf{z}_{i-1}$ and $\mathbf{z}_i$ axes. The generalized variable is $q_i = \theta_i$ for a revolute joint and $q_i = d_i$ for a prismatic joint.

The vector function $\mathbf{\Phi}(\mathbf{q}^*)$ characterizes the set of all points inside and on the boundary of the reach envelope generated by an anatomical landmark, and typically selected as a fingertip. The objective is to visualize this vector function consisting of many parameters and to better understand the motion governed by $\mathbf{\Phi}(\mathbf{q}^*)$. At a specified position in space given by $\mathrm{P}(x_p, y_p, z_p)$, Eq. 1 can be written as a constraint function.

$$\mathbf{\Omega}(\mathbf{q}^*) = \begin{bmatrix} x(\mathbf{q}^*) - x_p \\ y(\mathbf{q}^*) - y_p \\ z(\mathbf{q}^*) - z_p \end{bmatrix} = \mathbf{0} \tag{4}$$

Ranges of Motion

Ranges of motion are imposed in terms of inequality constraints in the form of $q_i^L \le q_i \le q_i^U$, where $i = 1, \ldots n$, are transformed into equalities by introducing a new set of generalized coordinates $\boldsymbol{\lambda} = [\lambda_1 \quad \ldots \quad \lambda_n]^T$ such that

$$q_i = (q_i^L + q_i^U)/2 + (q_i^U - q_i^L)/2 \sin\lambda_i \qquad i = 1, \ldots, n \tag{5}$$

where the new variable λ_i is inherently constrained by the sine function and does not change the dimensionality of the problem. In order to include the effect of the ranges of motion, it is proposed to augment the constraint equation $\mathbf{\Omega}(\mathbf{q}^*)$ with the parameterized ranges of motion, such that

$$\mathbf{H}(\mathbf{q}) = \begin{bmatrix} x(\mathbf{q}^*) - x_p \\ y(\mathbf{q}^*) - y_p \\ z(\mathbf{q}^*) - z_p \\ q_i - a_i - b_i \sin\lambda_i \end{bmatrix} = \mathbf{0} \quad i = 1, \ldots n$$

(6)

where $\mathbf{q} = \begin{bmatrix} \mathbf{q}^{*T} & \boldsymbol{\lambda}^T \end{bmatrix}^T$ is the vector of all generalized coordinates. Note that although $n-$new variables (λ_i) have been added, $n-$equations have also been added to the constraint vector function without loosing the dimensionality of the problem.

The *Jacobian* (after the German mathematician Karl Gustav Jacob Jacobi) of the constraint function $\mathbf{H}(\mathbf{q})$ at a point $\mathbf{q}^0$ is the $(3+n)\times 2n$ matrix

$$\mathbf{H}_{\mathbf{q}} = \partial \mathbf{H} / \partial \mathbf{q} \tag{7}$$

where the subscript denotes a derivative. With the modified formulation that includes ranges of motion, the Jacobian is expanded to

$$\mathbf{H}_{\mathbf{q}} = \left[\begin{array}{c|c} \boldsymbol{\Phi}_{\mathbf{q}^*} & \mathbf{0} \\ \hline \mathbf{I} & \mathbf{q}^*_{\boldsymbol{\lambda}} \end{array}\right] \tag{8}$$

where $\mathbf{q}^*_{\boldsymbol{\lambda}} = \partial \mathbf{q}^* / \partial \boldsymbol{\lambda}$, $\boldsymbol{\Phi}_{\mathbf{q}^*} = \partial \boldsymbol{\Phi} / \partial \mathbf{q}^*$, $\mathbf{0}$ is a $(3\times n)$ zero matrix, $\mathbf{I}$ is the identity matrix, and

$$\boldsymbol{\Phi}_{\mathbf{q}^*} = \begin{bmatrix} x_{q_1} & x_{q_2} & \ldots & x_{q_n} \\ y_{q_1} & y_{q_2} & \ldots & y_{q_n} \\ z_{q_1} & z_{q_2} & \ldots & z_{q_n} \end{bmatrix} \tag{9}$$

$$\mathbf{q}^*_{\lambda} = \begin{bmatrix} -((q_1^U - q_1^L)/2)\cos\lambda_1 & 0 & \ldots & 0 \\ 0 & -((q_2^U - q_2^L)/2)\cos\lambda_2 & \ldots & 0 \\ 0 & 0 & \ldots & 0 \\ 0 & 0 & \ldots & -((q_n^U - q_n^L)/2)\cos\lambda_n \end{bmatrix} \tag{10}$$

In earlier work by the authors aimed at determining difficulties in the control of robot manipulators (Abdel-Malek and Yeh 1997a; 1997b; Abdel-Malek, et al. 1997; and Abdel-Malek, et al. 1999), it was shown that impediments to motion (halting of a trajectory) arise inside the workspace when the Jacobian becomes singular (Abdel-Malek and Yeh 2000). Because the Jacobian is not square, rank deficiency criteria were developed. Before addressing these criteria, it is important to show why the singularity of the Jacobian has a direct effect on the control. The differentiation of Eq. (1) with respect to time yields the velocity of the fingertip $\dot{\boldsymbol{\Phi}}$ as

$$\dot{\boldsymbol{\Phi}} = \boldsymbol{\Phi}_{\mathbf{q}^*} \dot{\mathbf{q}}^* \tag{11}$$

where $\dot{\mathbf{q}}^*$ is the vector of joint velocities. Given a specified path trajectory (i.e., $\dot{\mathbf{\Phi}}$), the calculation of $\dot{\mathbf{q}}^*$ (i.e., joint velocities) requires computing an inverse of the Jacobian $\mathbf{\Phi}_{\mathbf{q}^*}$. For a singular Jacobian, it is not possible to compute the required velocities. These cases are typically associated with a kinematic configuration of the upper extremity that does not admit motion in a particular direction, but requires a change in the arm's posture in order to execute the path. If the Jacobian was square, then the determinant of $\mathbf{\Phi}_{\mathbf{q}^*}$ will yield the postures in space where singular behavior occurs. We will use this concept to explore the surrounding workspace.

Jacobian Analysis

Because the Jacobian is not square, we define these singular sets as a subset of the workspace in which the Jacobian of the constraint function of Eq. (7) is **row rank deficient** (Abdel-Malek, *et al*. 1999); i.e., the barriers are defined by ∂W and characterized by

$$\partial W \subset \left\{ \text{Rank } \mathbf{H}_{\mathbf{q}}(\mathbf{q}) < k, \text{ for some } \mathbf{q} \text{ with } \mathbf{H}(\mathbf{q}) = \mathbf{0} \right\} \tag{12}$$

where k is at least $(3+n-1)$. Imposition of the rank deficiency condition can be implemented using a variety of methods, but perhaps the most computationally efficient one is the repeated elimination of square sub-Jacobians, until a number of non-linear equations are determined. For example, consider a 7 DOF model of the arm, where the Jacobian is 10×14, where $\mathbf{\Phi}_{\mathbf{q}^*}$ is in the following form, $\begin{bmatrix} - & - & - & - & - & - & - \\ - & - & - & - & - & - & - \\ - & - & - & - & - & - & - \end{bmatrix}_{3\times7}$ and where $\mathbf{q}_{\lambda}^*$ is in this form: $\begin{bmatrix} - & - & - & - & - & - & - \\ - & - & - & - & - & - & - \\ - & - & - & - & - & - & - \\ - & - & - & - & - & - & - \\ - & - & - & - & - & - & - \\ - & - & - & - & - & - & - \\ - & - & - & - & - & - & - \end{bmatrix}_{7\times7}$ Therefore, three sets of singularities can be identified:

(a). The largest square submatrix of $\mathbf{\Phi}_{\mathbf{q}^*}$ is 3×3 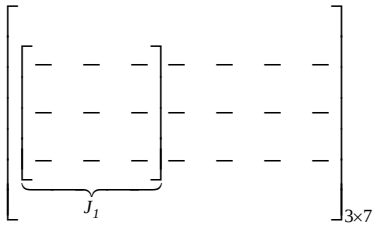 , …,

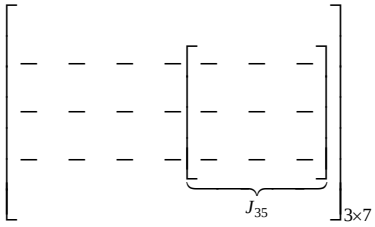 There are a total of $\frac{n!}{3!(n-3)!}=\frac{7!}{3!4!}=35$ submatrices (also called sub-Jacobians).. The determinants of these matrices are $|J_1|=\begin{vmatrix} - & - & - \\ - & - & - \\ - & - & - \end{vmatrix}$, …, $|J_{35}|=\begin{vmatrix} - & - & - \\ - & - & - \\ - & - & - \end{vmatrix}$. If all the determinants are kept at zero, then the group of equations can then be numerically solved to identify the singular sets.

(b). When q_i reaches its limit, eliminate the ith column in $\mathbf{\Phi}_{\mathbf{q}^*}$ and it will be a 3×6 matrix. Therefore there are 20 sub-Jacobians and 20 equations can be solved together to obtain the third set. When q_i and q_j reach their limits repeat the same procedure to find the singular set. When q_i, q_j and q_k reach their limits repeat the same procedure to find the singular set until the remaining Jacobian of $\mathbf{\Phi}_{\mathbf{q}^*}$ is a square matrix. These sets are denoted by **a**, **b**, and **c**, where each set comprises a number of constant joint values (from the total number of DOF) and two variables. Upon substituting these sets into Eq. (1), we obtain an equation of a surface parameterized in terms of two variables (i.e., a 2DOF surface in 3D space), such that:

$$\mathbf{f}^{(i)}(\mathbf{u}^{(i)})=\mathbf{\Phi}(\mathbf{u}^{(i)},\mathbf{q}^{+}) \tag{13}$$

where $\mathbf{q}^{+}\rightarrow\mathbf{q}^{*}\bigcap\mathbf{u}^{(i)}$ and $\mathbf{f}^{(i)}$ is the vector function describing the new parametric surface characterizing a barrier to motion.

(c). Since $\mathbf{q}_{\lambda}^{*}$ is a square matrix the singular sets can be obtained by solving the equation $\left|\mathbf{q}_{\lambda}^{*}\right| = \begin{vmatrix} - & - & - & - & - & - & - \\ - & - & - & - & - & - & - \\ - & - & - & - & - & - & - \\ - & - & - & - & - & - & - \\ - & - & - & - & - & - & - \\ - & - & - & - & - & - & - \\ - & - & - & - & - & - & - \end{vmatrix} = 0$. The singular sets are exact when the joints reach their limits.

In order to separate the analysis of rotational joints from that of translational joints, we break the formulation down into two distinct steps. First, we address the all-revolute 7 DOF model of the human upper extremity (including glenohumeral, elbow and wrist), but exclude the two shoulder translational joints. We will then perform a sweep of the resulting envelope to visualize the complete reach envelope.

Motion on the Barriers of Motion

To better understand when the hand may or may not cross barriers under given conditions, we explore the barrier's kinematic properties. We propose a criterion that is based on normal acceleration at a point on a barrier, such that crossability is achieved if the barrier admits a normal acceleration in one direction or another. A point on a barrier admits motion normal to the surface in either direction depending on the difference in acceleration components (defined by the indicator η), such that

$$\eta = a_n - \frac{v_t^2}{\rho_o} \tag{14}$$

where v_t is the tangential velocity, a_n is normal acceleration, and $1/\rho_o$ is the normal curvature of the barrier *with respect to the tangent direction* of v_t (ρ_o is the radius of curvature). The need for formulating the problem in terms of velocities and accelerations will become apparent, as the resulting expression for the indicator η will be independent of acceleration values, but will be a quadratic form that has definiteness properties. A point on a singular surface will have no acceleration if the quantity η computes to null.

For a singular parametric entity $\mathbf{f}^{(i)}(\mathbf{u}^{(i)}) \in \mathbf{R}^3$ (where $\mathbf{u}$ is a vector representing the remaining joint variables—those not constant), and in the field of differential geometry, the *First Fundamental Form* (Farin 1993) is denoted by $\mathbf{I}_p$, where $\mathbf{u}^{(i)} = \begin{bmatrix} u & v \end{bmatrix}^T = \begin{bmatrix} q_i & q_j \end{bmatrix}^T$, and is defined as

$$\mathbf{I}_p \equiv \delta\mathbf{u}^T \mathbf{f}_\mathbf{u}^T \mathbf{f}_\mathbf{u} \delta\mathbf{u} \tag{15}$$

where $\mathbf{f}_\mathbf{u} = \partial\mathbf{f}/\partial\mathbf{u}$. The *Second Fundamental Form* is defined as

$$\mathbf{II}_p \equiv \delta\mathbf{u}^T \left[\mathbf{N}^T \mathbf{f}\right]_{\mathbf{uu}} \delta\mathbf{u} \tag{16}$$

or expanded to

$$\mathbf{II}_p = \mathbf{N}^T \mathbf{f}_{uu} du^2 + 2\mathbf{N}^T \mathbf{f}_{uv} du\, dv + \mathbf{N}^T \mathbf{f}_{vv} dv^2 \tag{17}$$

where N is the vector normal to the singular surface and $\mathbf{f}_{uv} = \partial^2\mathbf{f}/\partial u \partial v$. The Normal Curvature K_o of a parametric surface at a configuration $\mathbf{q}_o$, in the direction of du/dv, can then be defined as the ratio (Farin 1993)

$$K_o = \frac{1}{\rho_o} = \frac{\mathbf{II}_p}{\mathbf{I}_p} \tag{18}$$

In order to determine the kinematics quantities, we define the *Time-Modified First and Second Fundamental Forms* as

$$\mathbf{I}'_p \equiv \dot{\mathbf{u}}^T \mathbf{f}_\mathbf{u}^T \mathbf{f}_\mathbf{u} \dot{\mathbf{u}} \tag{19}$$

$$\mathbf{II}'_p \equiv \dot{\mathbf{u}}^T \left[\mathbf{N}^T \mathbf{f}\right]_{\mathbf{uu}} \dot{\mathbf{u}} \tag{20}$$

such that the normal curvature can still be defined as

$$K_o = \frac{1}{\rho_o} = \frac{\mathbf{II}_p}{\mathbf{I}_p} = \frac{\mathbf{II}'_p}{\mathbf{I}'_p} \tag{21}$$

For a singular surface $\mathbf{f}^{(i)}(\mathbf{u}^{(i)})$, the derivative using the chain rule is $\mathbf{f}_\mathbf{u}\dot{\mathbf{u}}$. Similarly, for the overall description of the workspace $\mathbf{G}(\mathbf{q})$, the derivative is $\mathbf{G}_\mathbf{q}\dot{\mathbf{q}}$. Therefore, at an instant of time, the tangential velocity in terms of $\mathbf{f}$ or $\mathbf{G}$ at any point on the barrier is

$$\mathbf{v}_t = \mathbf{f}_\mathbf{u}\dot{\mathbf{u}} = \mathbf{G}_\mathbf{q}\dot{\mathbf{q}} \tag{22}$$

If joint limits are considered, then the derivatives can be written as $\dot{\mathbf{u}} = \mathbf{u}_s\dot{\mathbf{s}}$ and $\dot{\mathbf{q}} = \mathbf{q}_s\dot{\mathbf{s}}$. The squared norm of the velocity is

$$\left|\mathbf{v}_t\right|^2 = \mathbf{v}_t^T\mathbf{v}_t = \dot{\mathbf{u}}^T\mathbf{f}_\mathbf{u}^T\mathbf{f}_\mathbf{u}\dot{\mathbf{u}} \tag{23}$$

which is equal to the Time-Modified First Fundamental Form $\mathbf{I}'_p$ of Eq. 19. Therefore, $\mathbf{I}'_p$ can be written as

$$\mathbf{I}'_p = \left|v_t\right|^2 \tag{24}$$

Substituting $1/\rho_o$ into η yields

$$\eta = a_n - \left|v_t\right|^2 \frac{\mathbf{II}'_p}{\mathbf{I}'_p} = a_n - \mathbf{II}'_p \tag{25}$$

This expression can be written in quadratic form whereby the matrix of the quadratic form need only be evaluated.

4. Reach Envelope of the Upper Extremity Excluding Translation

Consider a model of the upper extremity comprising 7 rotational joints (7DOFs) as shown in Figure 5. Note that this model does not include the two translational joints in the shoulder, which will be addressed in the subsequent section. Note too that the arm is fully extended, as it was in the initial configuration. We will consider the following ranges of motion from this initial configuration: $-90^o \le q_3 \le 90^o$, $-110^o \le q_4 \le 120^o$, $-90^o \le q_5 \le 90^o$, $-150^o \le q_6 \le 0^o$, $-60^o \le q_7 \le 60^o$, $-20^o \le q_8 \le 20^o$, and $-90^o \le q_9 \le 90^o$.

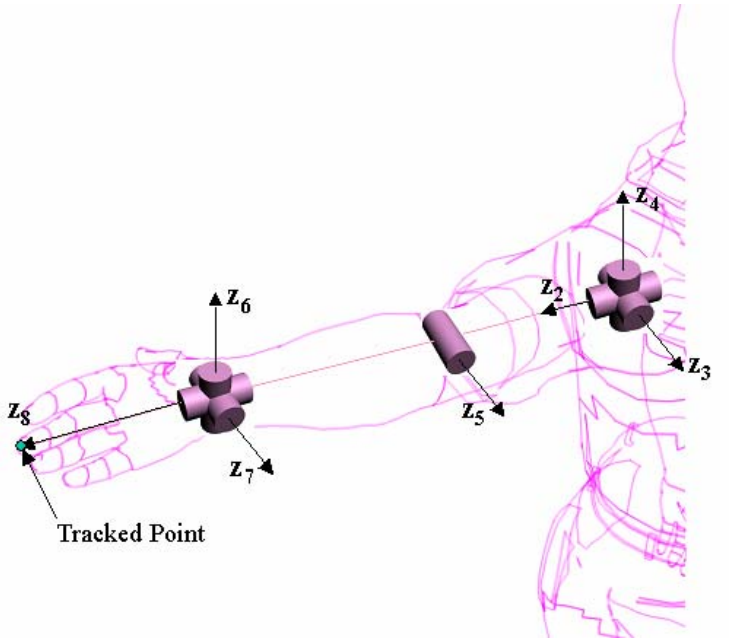

Figure 5. Kinematic model of the 7DOF all revolute upper extremity

According to the DH method, the XYZ coordinates of the tracked fingertip point in terms of the seven variables are

$$\begin{aligned}
\mathbf{\Phi}(\mathbf{q})[1] &= -20c_3c_5s_4 + 20s_3s_5 + 15c_6(-c_3c_5s_4 + s_3s_5) - 15c_3c_4s_6 + 10(c_8(c_7(c_6(-c_3c_5s_4 \\
&\quad + s_3s_5) - c_3c_4s_6) + (c_5s_3 + c_3s_4s_5)s_7) + (-c_3c_4c_6 - (c_3c_5s_4 + s_3s_5)s_6)s_8 \\
\mathbf{\Phi}(\mathbf{q})[2] &= -20c_5s_3s_4 - 20c_3s_5 + 15c_6(-c_5s_3s_4 - c_3s_5) - 15c_4s_3s_6 + 10(c_8(c_7(c_6(-c_5s_3s_4 \\
&\quad - c_3s_5) - c_4s_3s_6) + (-c_3c_5 + s_3s_4s_5)s_7) + (-c_4c_6s_3 - (-c_5s_3s_4 - c_3s_5)s_6)s_8 \\
\mathbf{\Phi}(\mathbf{q})[3] &= 20c_4c_5 + 15c_4c_5c_6 - 15s_4s_6 + 10(c_8(c_7(c_4c_5c_6 - s_4s_6) - c_4s_5s_7) \\
&\quad + (-c_6s_4 - c_4c_5s_6)s_8)
\end{aligned} \tag{26}$$

Singularity Sets

Since $\mathbf{\Phi}_{\mathbf{q}^*}$ is a 3×7 matrix, there are $\frac{n!}{3!(n-3)!} = \frac{7!}{3!4!} = 35$ equations to be simultaneously solved, which represent the determinants of all square 3◈3 sub-Jacobians. There are three sets of solutions:

(a). As a result of solving the equations generated by the sub-Jacobians, the rank deficiency of $\mathbf{\Phi}_{\mathbf{q}^*}$ yields $s_1 = \{q_6 = 0, q_7 = 0, q_8 = 0\}$. This set, when substituted into Eq. 1 yields a surface parameterized into three generalized coordinates.

(b). The second set is identified when one, two or three joints reach their limits (in this example, $\mathbf{\Phi}(\mathbf{q})$ only includes 6 variables, $q_3,...,q_8$). When one joint reaches an upper or lower limit, for example $q_4 = 2\pi/3$, we substitute $q_4 = 2\pi/3$ into $\mathbf{\Phi}(\mathbf{q})$ and compute $\mathbf{\Phi}_{\mathbf{q}^*}$ (the remaining Jacobian excluding the q_4 column). Since $\mathbf{\Phi}_{\mathbf{q}^*}$ is a 3×6 matrix, there are $\frac{6!}{3!3!} = 20$ equations to be simultaneously solved, whose solution is $\hat{\mathrm{a}} = \{q_5 = 0, q_7 = 0, q_8 = 0\}$. Therefore, a singular set is identified as $\mathbf{a}_1 = \{q_4 = \frac{2\pi}{3}, q_5 = 0, q_7 = 0, q_8 = 0\}$. Substituting only one of the constraint limits and applying the rank-deficiency condition yields the singular sets listed in Appendix A. This process continues for all variables. When two variables reach their constraint limits, such as $q_3 = -\pi/2, q_4 = 2\pi/3$, substituting these limits into $\mathbf{\Phi}(\mathbf{q})$ and calculating $\mathbf{\Phi}_{\mathbf{q}^*}$ (again, excluding both associated columns) yields 4 equations. When simultaneously solved we obtain $\hat{\mathrm{b}} = \{q_7 = 0, q_8 = 0\}$. Therefore a singular set is identified as $\mathbf{b}_2 = \{q_3 = -\pi/2, q_4 = 2\pi/3, q_7 = 0, q_8 = 0\}$. Repeating the process also yields the singular sets listed in Appendix A. When three variables reach their constraint limits such as $q_3 = -\frac{\pi}{2}, q_4 = -\frac{11\pi}{18}, q_5 = -\frac{\pi}{2}$, substituting these limits into $\mathbf{\Phi}(\mathbf{q})$ and calculating $\mathbf{\Phi}_{\mathbf{q}^*}$ (again, excluding three associated columns) yields 1 equation. When solved, we obtain $\hat{\mathrm{c}} = \{q_8 = 0\}$. Therefore a singular set is identified as $\mathbf{c}_1 = \{q_3 = -\frac{\pi}{2}, q_4 = -\frac{11\pi}{18}, q_5 = -\frac{\pi}{2}, q_8 = 0\}$.

(c). The third set is when four of the variables reach their constraint limits such as $q_3 = \begin{Bmatrix} -\pi/2 \\ \pi/2 \end{Bmatrix}$, $q_4 = \begin{Bmatrix} -11\pi/18 \\ 2\pi/3 \end{Bmatrix}$, $q_5 = \begin{Bmatrix} -\pi/2 \\ \pi/2 \end{Bmatrix}$, and $q_6 = \begin{Bmatrix} -5\pi/6 \\ 0 \end{Bmatrix}$. There are total 232 singular surfaces in Appendix A. In order to perform this symbolic manipulation, we have developed a computer code using Mathematica®.

The determinants of sub-Jacobians for $\mathbf{\Phi}(\mathbf{q})$ are as follows:

$$|J_1| = |J_2| = \cdots = |J_{16}| = 0$$

$$|J_{17}| = 500((2+\cos q_7 \cos q_8)\sin q_6 + \cos q_6 \sin q_8)(-\cos q_8 \sin q_4 \sin q_5 \sin q_7 + \cos q_4((2 + \cos q_7 \cos q_8)\sin q_6 + \cos q_6 \sin q_8) + \cos q_5 \sin q_4(4 + \cos q_6(2+\cos q_7 \cos q_8) - \sin q_6 \sin q_8))$$

.

.

.

$$|J_{29}| = |J_{30}| = 250\cos q_8(2\cos q_5 \cos q_7 + \sin q_5 \sin q_7)((2+\cos q_7 \cos q_8)\sin q_6 + \cos q_6 \sin q_8)$$

$$|J_{31}| = -250\cos q_8(\cos q_8 \sin q_5 \sin q_6 \sin q_7 + \cos q_5(2\cos q_7 \cos q_8 \sin q_6 + \sin q_8 + 2\cos q_6 \sin q_8))$$

$$|J_{32}| = 250\cos q_8 \sin q_7(4 + 2\cos q_7 \cos q_8 + \cos q_6(2+\cos q_7 \cos q_8) - \sin q_6 \sin q_8)$$

$$|J_{33}| = 125\sin q_8(2(1+\cos q_6)(\cos q_7)^2 \cos q_8 + (-3+\cos(2q_7))\cos q_8 + 2\cos q_7(4 + 2\cos q_6 - \sin q_6 \sin q_8))$$

$$|J_{34}| = -250(2+\cos q_6)(\cos q_8)^2 \sin q_7$$

$$|J_{35}| = -125\sin(2q_8)$$

Enforce all above to be zero and solve the equations simultaneously and one obtains the rank deficiency of $\mathbf{\Phi}_{\mathbf{q}^*}$ which is $s_1 = \{q_6 = 0, q_7 = 0, q_8 = 0\}$.

When q_i reaches its limit, such as $q_3 = -\frac{\pi}{2}$, we substitute $q_3 = -\pi/2$ into $\mathbf{\Phi}(\mathbf{q})$ and compute $\mathbf{\Phi}_{\mathbf{q}^*}$ (the remaining Jacobian excluding the q_3 column). The determinants of the sub-Jacobians are

$$|J_1| = |J_2| = \cdots = |J_{10}| = 0$$

$$|J_{11}| = -500((2+\cos q_7 \cos q_8)\sin q_6 + \cos q_6 \sin q_8)(-\cos q_8 \sin q_5 \sin q_7 + \cos q_5(4+\cos q_6(2+\cos q_7 \cos q_8) - \sin q_6 \sin q_8))$$

$$|J_{12}| = -250(1+2\cos q_6)\cos q_8 \sin q_5(-\cos q_8 \sin q_5 \sin q_7 + \cos q_5(4+\cos q_6(2+\cos q_7 \cos q_8) - \sin q_6 \sin q_8))$$

$$|J_{13}| = -250(2\cos q_8 \sin q_6 + (1+2\cos q_6)\cos q_7 \sin q_8)(-\cos q_8 \sin q_5 \sin q_7 + \cos q_5(4+\cos q_6 (2+\cos q_7 \cos q_8) - \sin q_6 \sin q_8))$$

$$|J_{14}| = 250\cos q_8(2\cos q_5 \cos q_7 + \sin q_5 \sin q_7)((2+\cos q_7 \cos q_8)\sin q_6 + \cos q_6 \sin q_8)$$

$$|J_{15}| = 250(\cos q_7 \sin q_5 - 2\cos q_5 \sin q_7)\sin q_8((2+\cos q_7 \cos q_8)\sin q_6 + \cos q_6 \sin q_8)$$

$$|J_{16}| = -125(2(\cos q_8)^2 \sin q_5 \sin q_6 \sin q_7 + \cos q_5(4\cos q_7(\cos q_8)^2 \sin q_6 + (1+2\cos q_6)\sin(2q_8)))$$

$$|J_{17}| = 250\cos q_8 \sin q_7(4+2\cos q_7 \cos q_8 + \cos q_6(2+\cos q_7 \cos q_8) - \sin q_6 \sin q_8)$$

$$|J_{18}| = 125\sin q_8(2(1+\cos q_6)(\cos q_7)^2 \cos q_8 + (-3+\cos(2q_7))\cos q_8 + 2\cos q_7(4+2\cos q_6 - \sin q_6 \sin q_8))$$

$$|J_{19}| = -125\sin(2q_8)$$

$$|J_{20}| = -250(2+\cos q_6)(\cos q_8)^2 \sin q_7$$

If we enforce the rule that all the determinants will be zero simultaneously and solve these equations, we obtain one singular set, $\mathbf{a}_5 = \{q_3 = \frac{\pi}{2}, q_5 = -\frac{\pi}{2}, q_7 = 0, q_8 = 0\}$. One can then obtain other $\mathbf{a}_i$ by repeating this procedure. When q_i and q_j reach their limits, such as $q_3 = -\frac{\pi}{2}$ and $q_4 = -\frac{11\pi}{18}$, we substitute them into $\mathbf{\Phi}(\mathbf{q})$ and compute $\mathbf{\Phi}_{\mathbf{q}^*}$ (the remaining Jacobian excluding the q_3 and q_4 columns). The determinants of the sub-Jacobians are

$$|J_1| = |J_2| = \cdots = |J_6| = 0$$

$$|J_7| = 250\cos q_8 \sin q_7(4+2\cos q_7 \cos q_8 + \cos q_6(2+\cos q_7 \cos q_8) - \sin q_6 \sin q_8)$$

$$|J_8| = 125\sin q_8(2(1+\cos q_6)(\cos q_7)^2 \cos q_8 + (-3+\cos(2q_7))\cos q_8 + 2\cos q_7(4+2\cos q_6 - \sin q_6 \sin q_8))$$

$$|J_9| = -250(2+\cos q_6)(\cos q_8)^2 \sin q_7$$

$$|J_{10}| = -125\sin(2q_8)$$

Once again, we enforce all of the determinants to be zero simultaneously and solve these equations to obtain one singular set $\mathbf{b}_1 = \{q_3 = -\frac{\pi}{2}, q_4 = -\frac{11\pi}{18}, q_7 = 0, q_8 = 0\}$. By repeating this procedure other $\mathbf{b}_i$ are obtained. When q_i, q_j and q_k reach their limits, such as $q_3 = -\frac{\pi}{2}$, $q_4 = -\frac{11\pi}{18}$ and $q_5 = -\frac{\pi}{2}$, we substitute them into $\mathbf{\Phi}(\mathbf{q})$ and compute $\mathbf{\Phi}_{\mathbf{q}^*}$ (the remaining Jacobian excluding the q_3, q_4 and q_5 columns). The determinants of sub-Jacobians are

$|J_1| = |J_2| = |J_3| = 0$

$|J_4| = -125\sin(2q_8)$

We enforce all the determinants to be zero simultaneously and solve these equations to obtain one singular set $\mathbf{c}_1 = \{q_3 = -\frac{\pi}{2}, q_4 = -\frac{11\pi}{18}, q_5 = -\frac{\pi}{2}, q_8 = 0\}$. We repeat this procedure to obtain other $\mathbf{c}_i$.

When $\mathbf{q}_{\lambda}^*$ is singular, then $\left|\mathbf{q}_{\lambda}^*\right| = -\frac{115\pi^7 \cos\lambda_3 \cos\lambda_4 \cos\lambda_5 \cos\lambda_6 \cos\lambda_7 \cos\lambda_8 \cos\lambda_9}{419904} = 0$.

We can obtain λ_i and plug it into Eq. 5; that means q_i reaches its limit. While $\mathbf{\Phi}(\mathbf{q})$ doesn't include q_9 when any four of the variables reach their limits, it will be singular set. It is now possible to visualize each surface by substituting all singular sets into Eq. 26, as illustrated in Figure 6.

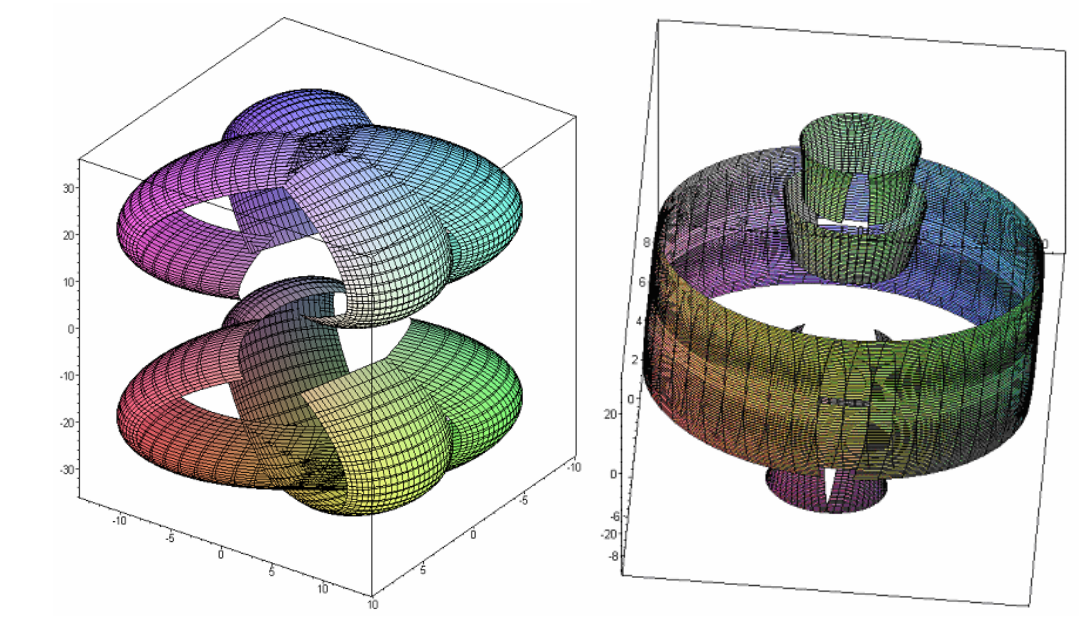

$\gamma_{41} - \gamma_{56}$ $\gamma_{153} - \gamma_{168}$

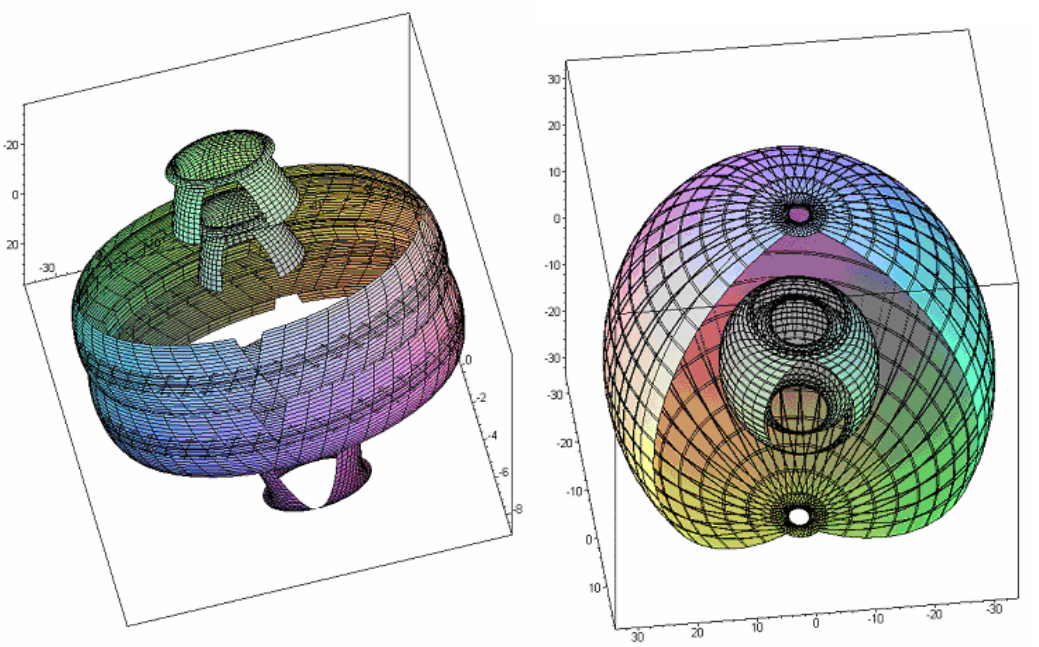

$\gamma_{169} - \gamma_{184}$ $\gamma_{201} - \gamma_{216}$

Figure 6. The different singular sets of surfaces

In fact, combining all singular surfaces yields the reach envelope of the 7 DOF model as shown in Figure 7. We have identified the outer boundary to the reach envelope in closed form (also shown in Figure 8).

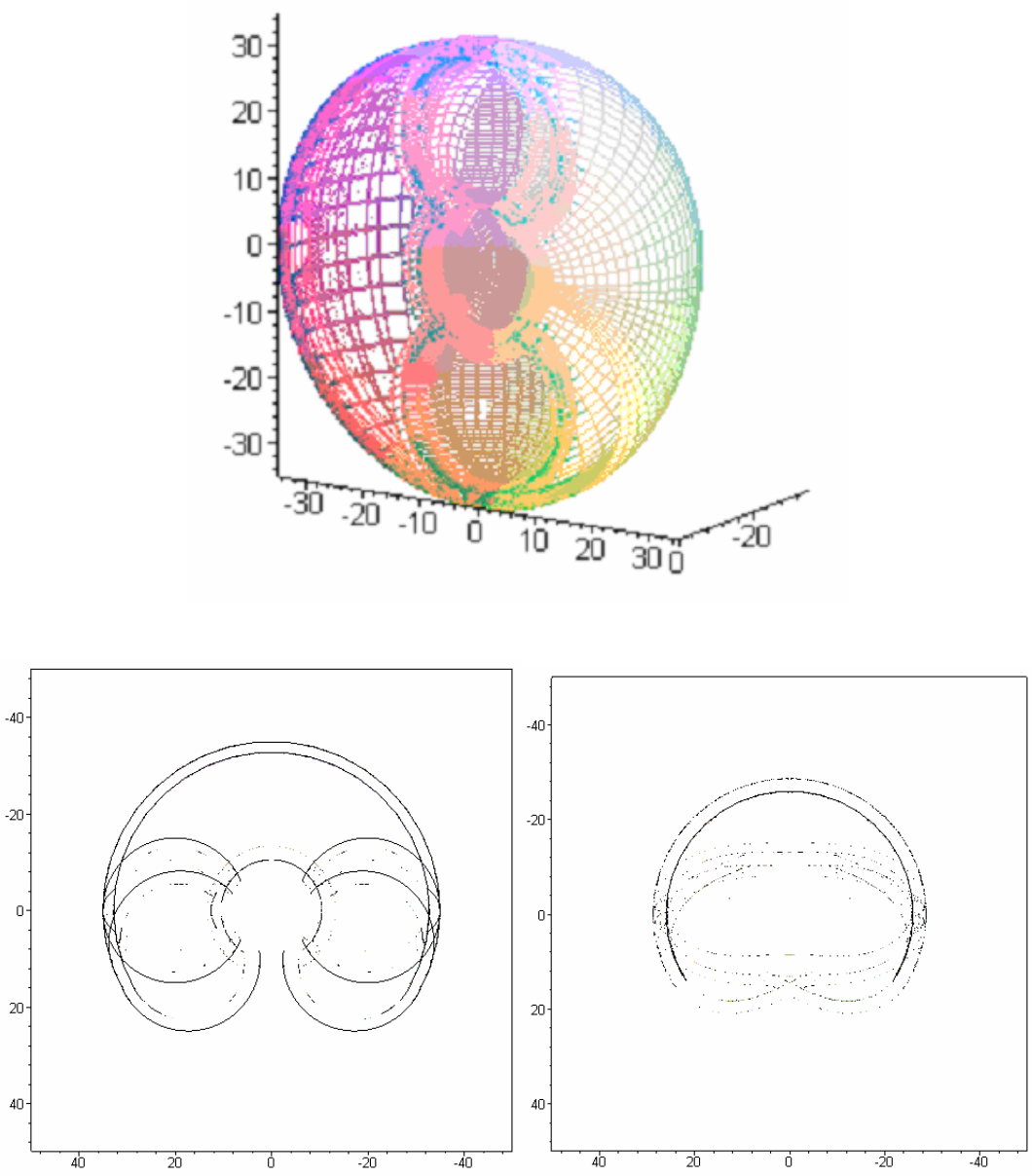

Figure 7. The cross section view of workspace for human arm model (7 DOF) and cross sections

at $z = 0$ and $z = 20$

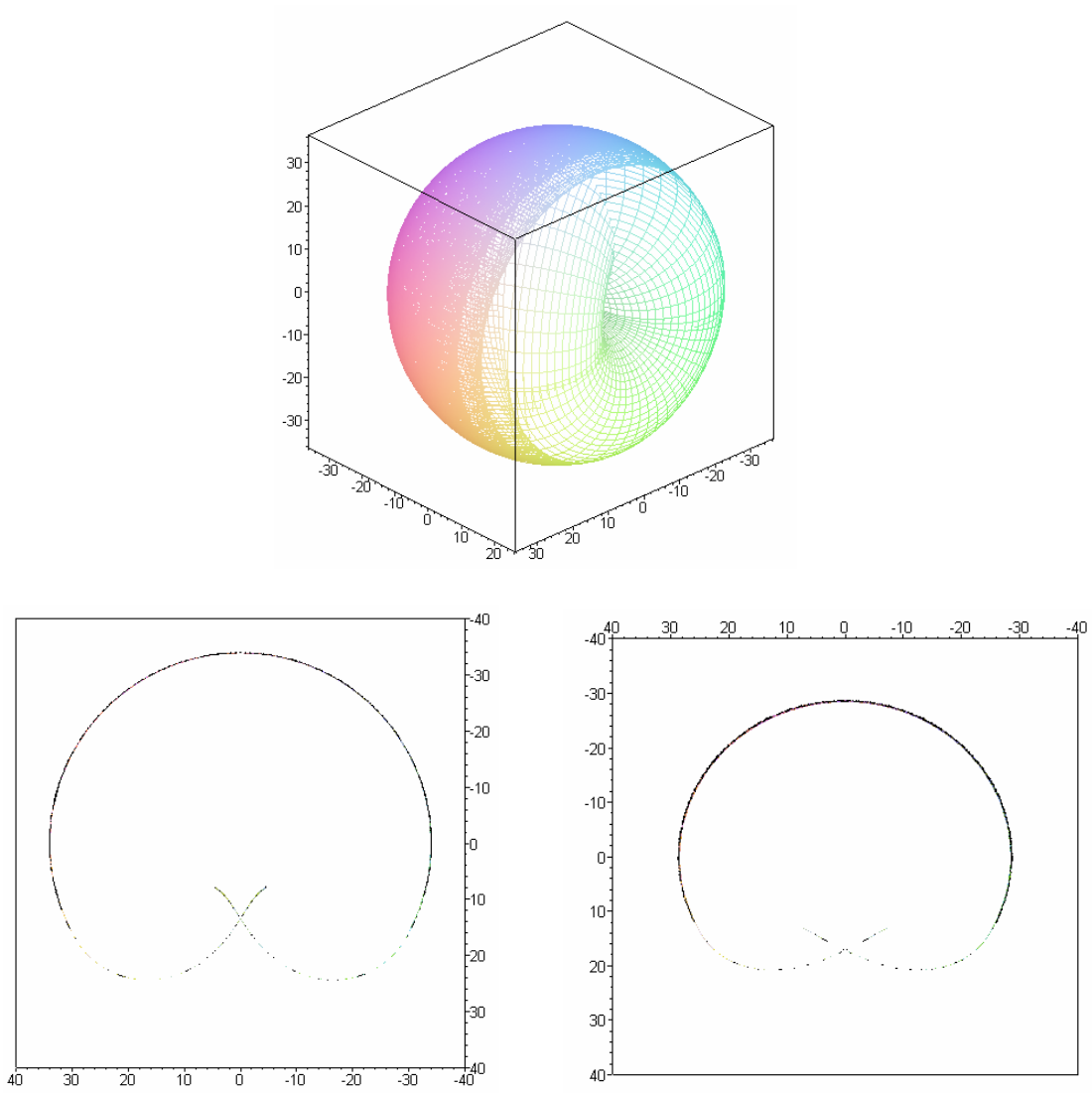

Figure 8. Envelope of the 7 DOF Model for Human Model and the cross sections at $z = 0$ and $z = 20$

5. Sweeping the 7-DOF in two translational directions

The effect of the scapula-thorasic translational motion is accounted for using a swept volume analysis (Blackmore, *et al.* 1999). We now include two translational joints to the shoulder complex, where the kinematic model of a 9 DOF upper extremity is shown in Figure 9.

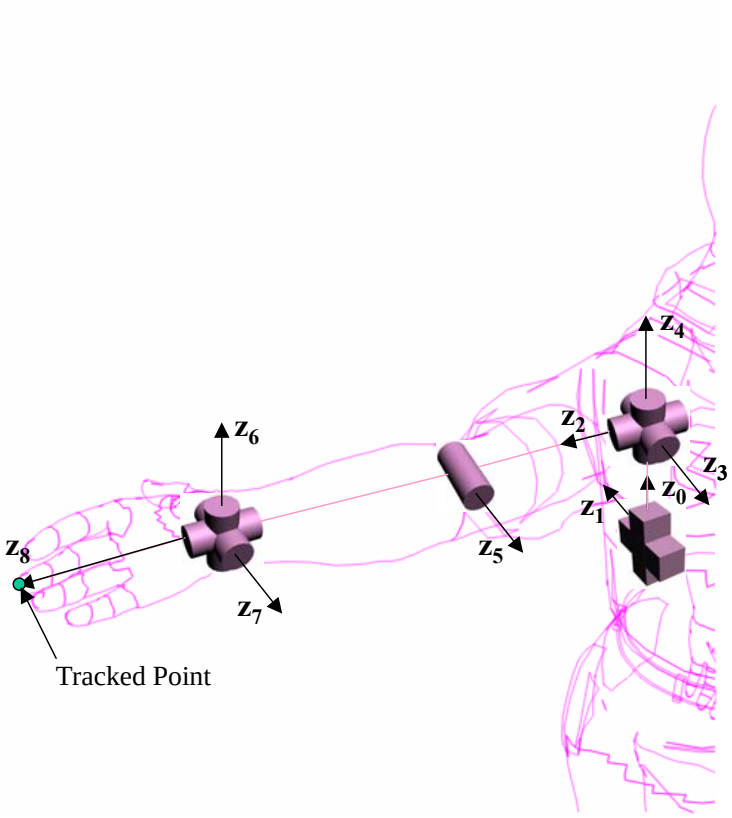

Figure 9. Kinematic model for 9 DOF Human Arm

There are a number of surface patches that constitute the outer boundary. These surfaces will be denoted by $\mathsf{F}_i(\hat{\mathbf{q}})$, where $i = 1,...,m$, m is the number of surface patches, and $\hat{\mathbf{q}} = \left[q_i, q_j \right]^T$ has no more than two variables for each surface patch. A sweep operation in the direction of $\boldsymbol{\psi}(q_1, q_2) = \left[q_1 \quad q_2 \quad 0 \right]^T$ (the two translational directions) with no rotation is defined by the sweep equation

$$\underbrace{\boldsymbol{\Gamma}(\mathbf{p})}_{\text{Swept volume}} = \mathbf{R} \underbrace{\boldsymbol{\Phi}_i(\hat{\mathbf{q}})}_{\text{Swept entity}} + \underbrace{\boldsymbol{\psi}(q_1, q_2)}_{\text{Translational path}} \tag{27}$$

where the rotation matrix $\mathbf{R}$ is $\mathbf{I}$, an identity matrix since no changes occur in its orientation. $\mathbf{p} = \left[q_1, q_2, u, v \right]^T$ now contains four variables for each surface (Figure 10), where u and v are the parametric variables of the surface patch on the boundary of the 7 DOF reach envelope.

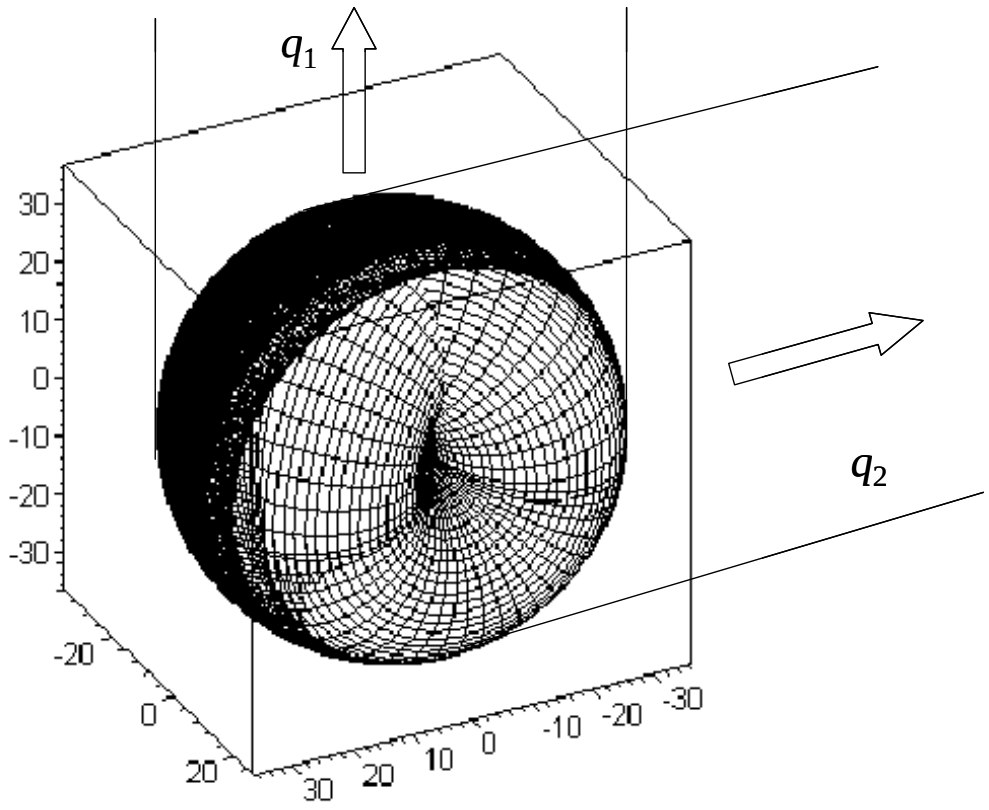

Figure 10. Sweeping of the 7DOF outer boundary in two translational directions

In order to visualize this vector function $\mathbf{\Gamma}(\mathbf{p})$, we again make use of the rank deficiency condition, where the Jacobian $\partial\mathbf{\Gamma}/\partial\mathbf{p}$ is a 3×4 matrix. The four determinants of the sub-Jacobians of $\partial\mathbf{\Gamma}/\partial\mathbf{p}$ are set to zero and singular sets are determined. As an example, consider the sweep of the surface patch defined by $\mathbf{\Phi}(u,v)=\begin{bmatrix}35\cos(u)\cos(v)\\35\cos(u)\sin(v)\\35\sin(v)\end{bmatrix}$ and characterized by the equation

$\mathbf{\Gamma}(\mathbf{p})=\begin{bmatrix}q_1+35\cos(u)\cos(v)\\q_2+35\cos(u)\sin(v)\\35\sin(v)\end{bmatrix}$, where $0\le u\le 2\pi$, $-\theta\le v\le \pi/2$, $-1.5\le q_1\le 1.5$ and $-1.5\le q_2\le 1.5$.

The Jacobian matrix is $\mathbf{\Gamma}_{\mathbf{p}} = \begin{bmatrix} 1 & 0 & -35\cos(v)\sin(u) & -35\cos(u)\sin(v) \\ 0 & 1 & -35\sin(u)\sin(v) & 35\cos(u)\cos(v) \\ 0 & 0 & 0 & 35\cos(v) \end{bmatrix}$. Singular sets have been determined with the following values: $\varsigma_1 = \{u = 0, v = \pi/2\}$, $\varsigma_2 = \{u = \pi, q_1 = -1.5\}$, $\varsigma_3 = \{u = 0, q_1 = 1.5\}$, $\varsigma_4 = \{u = 3\pi/2, q_2 = -1.5\}$, $\varsigma_5 = \{u = \pi/2, q_2 = 1.5\}$, and $\varsigma_6 = \{v = 0, q_2 = -1.5\}$. These sets are automatically substituted into $\mathbf{\Gamma}(\mathbf{p})$ to visualize the boundary. The process is repeated for all surface patches, and the resulting reach envelope is shown in Figure 11.

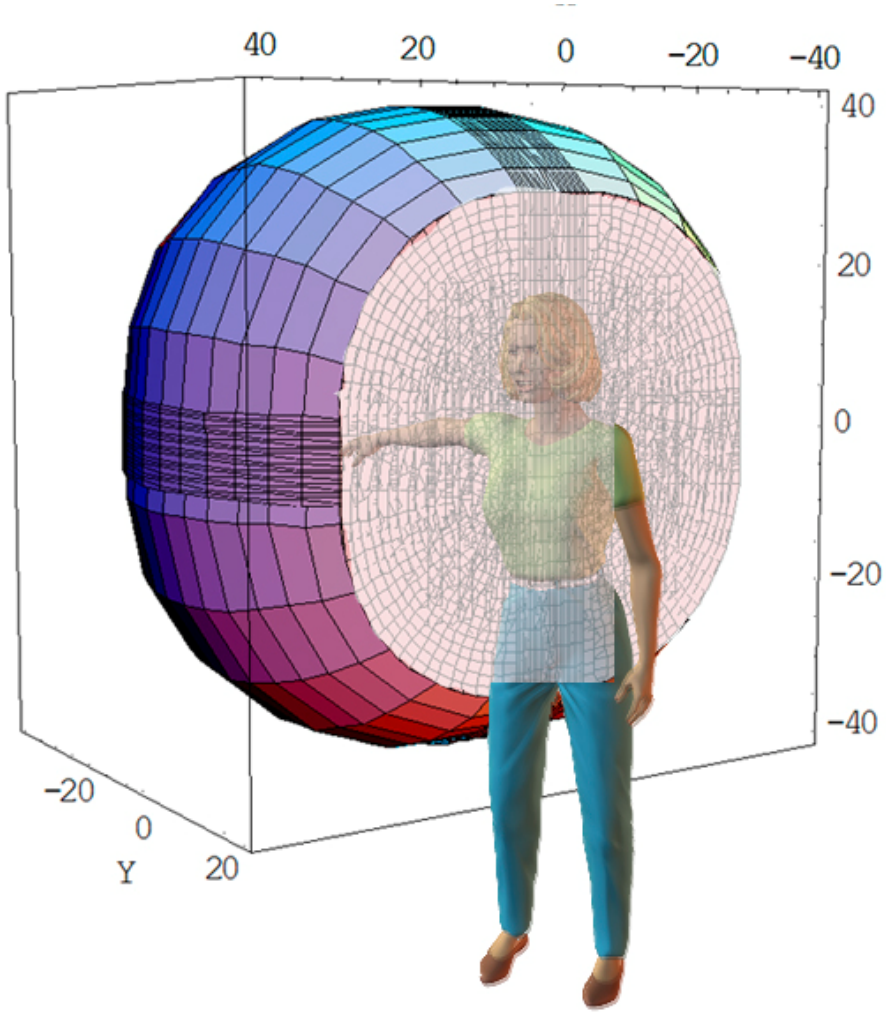

Figure 11. The final envelope of 9 DOF human arm model

Barriers to Motion

To better understand the relation between barriers within the reach envelope and the physical meaning of a singular configuration, we examine a singular set characterized by $\mathbf{a} = \{q_1 = 0, q_2 = 0, q_3 = 0, q_6 = -\frac{5\pi}{6}, q_7 = -\pi/3, q_8 = -\pi/9, q_9 = 0\}$, as shown in Figure 12 with the configurations ($q_4 = -\frac{\pi}{18}, q_4 = 0, q_4 = \frac{\pi}{12}$). In this case, there is no translational motion of the scapula thorasic motion; however, the elbow is at the limit $q_6 = -\frac{5\pi}{6}$, and the wrist joint has reached a combination of limits ($q_7 = 0, q_8 = -\pi/9, q_9 = 0$). Figure 13 shows the configurations of three singular sets $q_5 = -\frac{\pi}{12}$, $q_5 = 0$, and $q_5 = \frac{\pi}{12}$.

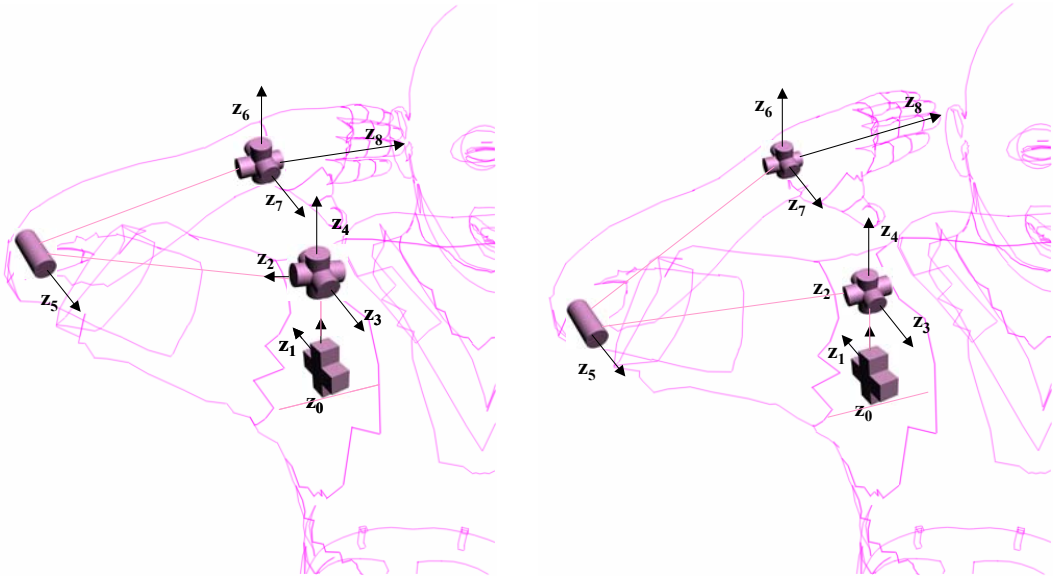

(a). $q_4 = -\frac{\pi}{18}$ (b). $q_4 = 0$

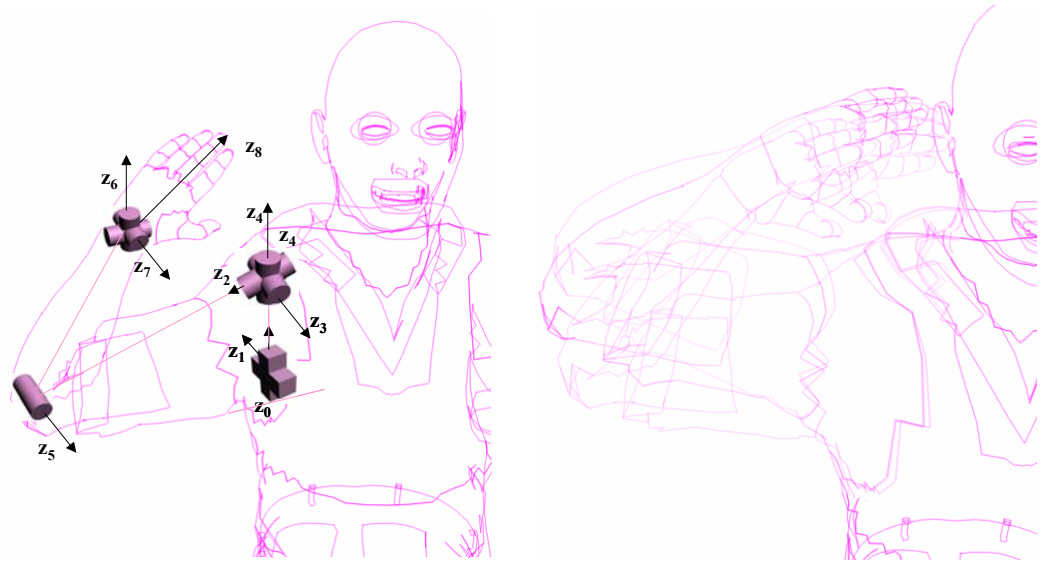

(c). $q_4 = \frac{\pi}{12}$ (d) Combined together

$(q_4 = -\frac{\pi}{18}, q_4 = 0, q_4 = \frac{\pi}{12})$

Figure 12. Configurations of three singular sets

Figure 13. Three configurations combined together ($q_5 = -\frac{\pi}{12}, q_5 = 0, q_5 = \frac{\pi}{12}$)

The Jacobian analysis has yielded seven constant values of the joint variables, but has left two variables unspecified (q_4, q_5). Substituting the set of constant variables into Eq. 27 yields a new equation parameterized in terms of the two remaining variables as

$$\mathbf{\Gamma}(q_4, q_5) = \begin{bmatrix} \frac{5}{2}(8 - 3\sqrt{3} + 2\cos(\frac{11\pi}{18}) - 2\sqrt{3}\sin(\frac{11\pi}{18}))\sin(q_5) \\ \frac{5}{2}(\cos(q_4)\cos(q_5)(-8 - 3\sqrt{3} + 2\cos(\frac{11\pi}{18}) - 2\sqrt{3}\sin(\frac{11\pi}{18})) - (3 + 2\sqrt{3}\cos(\frac{11\pi}{18}) + 2\sin(\frac{11\pi}{18}))\sin(q_4) \\ \frac{5}{2}(\cos(q_4)(3 + 2\sqrt{3}\cos(\frac{11\pi}{18}) + 2\sin(\frac{11\pi}{18})) + \cos(q_5)(8 - 3\sqrt{3} + 2\cos(\frac{11\pi}{18}) - 2\sqrt{3}\sin(\frac{11\pi}{18}))\sin(q_4) \end{bmatrix}$$

Note that the above expression represents the sweep of the fingertip in space with all joints but q_4, q_5 in a locked position. We plot this 2DOF surface in 3D space, as shown in Figure 14.

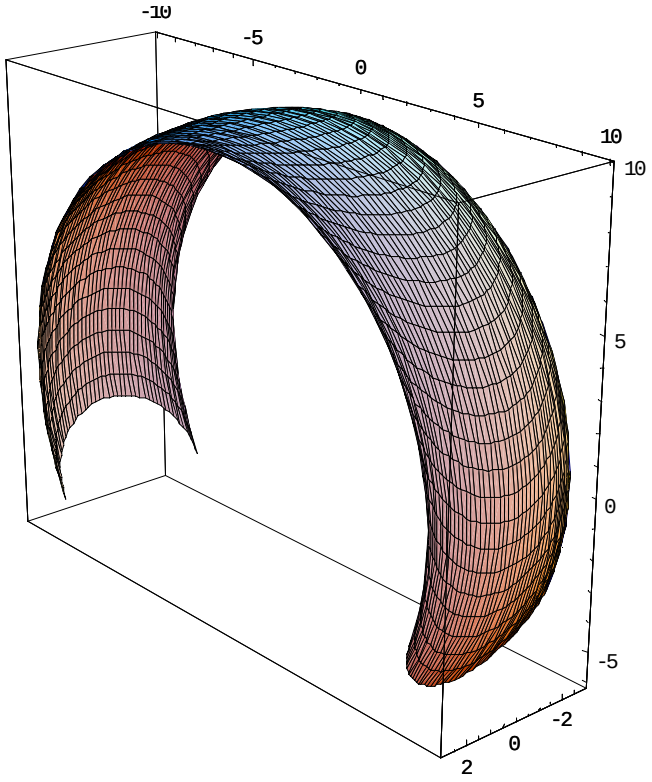

Figure 14. A barrier due to singular set

$$\mathbf{a} = \{q_1 = 0, q_2 = 0, q_3 = 0, q_6 = -\frac{5\pi}{6}, q_7 = -\pi/3, q_8 = -\pi/9, q_9 = 0\}$$

The physical significance of this surface can be observed by examining the inverse kinematic solution on any point on the surface. This particular configuration characterizing the barrier delineates important properties of the reach envelope.

To explain this physical behavior typically associated with Jacobian and limit singularities, consider the motion of one's arm aimed at reaching (with the fingertip) a point on the barrier surface (Figure 7), where many joints have reached their limits (or have reached a Jacobian) singularity, and some joints are free to move. For a given configuration with the fingertip at this point, it is not possible to admit motion normal to the barrier in at least one direction. However, the barrier is indeed in the reachable workspace; therefore, any point to the left and right of this point are reachable. This means that a different configuration (other than the configuration that yields the barrier), may allow the fingertip to admit motion across the barrier. Such a result has also been observed with mechanical manipulators (especially in the field of welding), where continuous motion of the end-effector is necessary. If the weld seam is positioned across a barrier, the manipulator may not smoothly execute the motion, but may halt, change inverse solutions, and then continue the motion. We believe that such kinematically-driven behavior of the upper extremities is important in identifying disabilities in issuing motor commands, and could play an important role in identifying such disabilities.

6. Conclusions

A 9 degree of freedom biomechanical model of the upper extremity has been developed, and was used to generate the reach envelope. We have presented a rigorous formulation for modeling, analysis, and visualization of the envelope and barriers where one or more joints have reached their limits or where a Jacobian singularity is identified. Fundamental to this formulation is the underlying concept of accounting for joint ranges

of motion in terms of inequality constraints imposed on the motion. It was shown that rank deficiency conditions of the Jacobian of the model yield surface patches that belong to the envelope. It was also shown that a subset of these surfaces fall on the boundary. Translational joints of the shoulder are accounted for using a swept volume approach, which yields closed form equations of the boundary. Furthermore, barriers within the reach envelope are important in explaining and verifying hand trajectories. Barriers that are a result of kinematic singularities present obstacles to motion for the upper extremity when encountered during a path, requiring that the motion be halted and switched to another posture. We believe that the identification of these barriers will aid in better understanding motor commands issued by the central nervous system, as well as perhaps providing insight into path following for people with disabilities.

This study is the first step towards a more rigorous investigation of the reachable workspace; a forthcoming extension of this work is to include upper extremity orientation capabilities to better understand human dexterity. Also underway is a study to relate barriers that appear within the workspace to neurological commands and motor skills.

7. Acknowledgements

This research was funded by the U.S.-Egypt Joint Science and Technology Board, a research initiation grant from the Society of Manufacturing Engineers (SME), and an award from the Iowa Space Grant Consortium and the US Army TACOM.

8. References

Abdel-Malek, K. and Yeh, H.J., 1997a, “Analytical Boundary of the Workspace for General Three Degree-of-Freedom Mechanisms,” *International Journal of Robotics Research.* Vol. 16, No. 2, pp. 198-213.

Abdel-Malek, K. and Yeh, H.J., 1997b, "Path Trajectory Verification for Robot Manipulators in a Manufacturing Environment" *IMechE Journal of Engineering Manufacture*, Vol. 211, pp. 547-556.

Abdel-Malek, K., Adkins, F., Yeh, H.J., and Haug, E.J., 1997, “On the Determination of Boundaries to Manipulator Workspaces,” *Robotics and Computer-Integrated Manufacturing, Vol. 13, No. 1, pp.63-72.*

Abdel-Malek, K., Yeh, H-J, and Khairallah, N., 1999, "Workspace, Void, and Volume Determination of the General 5DOF Manipulator, *Mechanics of Structures and Machines*, 27(1), 91-117.

Abdel-Malek, K., Yeh, H.J., and Othman, S. (1998) Swept Volumes, Void and Boundary Identification", *Computer Aided Design*, Vol. 30, Vol. 13, pp. 1009-1018.

Abdel-Malek, K.and Yeh, H.J., (2000), "Crossable Surfaces of Robotic Manipulators with Joint Limits", *ASME Journal of Mechanical Design*, Vol. 122, No. 1, March 2000, pp. 52-61.

Abdel-Malek, K., Yang, J., Brand, R., and Tanbour, E., "Towards Understanding the Workspace of The Upper Extremities," *Proceedings of 2001 SAE Digital Human Modeling for Design and Engineering*, 2001-01-2095, June 26-28, Arlington, VA, USA.

Benati, A. E., Gaglio, S., Tagliasco, V., Zaccaria, R., 1980, "Anthropomorfic robotics," *Biological Cybernetic*s, Vol. 38, pp. 125-140.

Denavit, J., and Hartenberg, R.S., 1955, "A Kinematic Notation for Lower-pair Mechanisms Based on Matrices," *Journal of Applied Mechanics, ASM*E, Vol. 22, pp. 215-221.

Dvir, Z., Berme, N. 1978, "The shoulder complex in elevation of the arm: a mechanism approach," *J. Biomechanics* 11, 219-225.

E.Y.S. Chao, J.D. Lynch, M.J. Vanderploeg (1993), "Simulation and Animation of Musculoskeletal Joint Systems", *Journal of Biomechanical Engineerin*g, Vol. 115, pp. 562-568, November 1993.

Engin ,A.E. (1984), "On the Theoretical Modeling of Human Joints", in *Mathematical Modelling in Science and Technology* (ed. J. R. Avula), Pergamon Press, New York, pp. 560–565.

Engin ,A.E. and S.T. Tumer (1989a), "Three-Dimensional Kinematic Modeling of the Human Shoulder Complex – I. Physical Model and Determination of Joint Sinus Cones", *Journal of Biomechanical Engineerin*g, 111, 107–112.

Engin ,A.E. and ST. Tumer (1989), "Three-Dimensional Kinematic Modeling of the Human Shoulder Complex – II. Mathematical Modelling and Solution via Optimization", *Journal of Biomechanical Engineerin*g, 111, 113–121.

Engin, A.E., "Kinematics of human shoulder motion," *Biomechanics od Diarthrotrial Joints*, Springer-Verlag, New York, 1990.

Farin, Gerald, Curves and Surfaces for CAGD, A Practical Guide, Academic Press, 1988.

Helm,F.C.T. van der (1994), "A Finite Element Musculoskeletal Model of the Shoulder Mechanism", *Journal of Biomechanic*s, 27, 551–569.

Högfors, C., B. Peterson, G. Sigholm, P. Herberts (1991), "Biomechanical Model of the Human Shoulder Joint", *J. Biomechanic*s, 24, 699–709.

Jackson, K.M., Joseph, J. and Wyard, S. J., 1977, "Sequential muscular contraction," *J. Biomechanics* 10, 97-100.

Lenarcic, J. and Umek, A., "Simple model of human arm reachable workspace," *IEEE Transactions on Systems, Man, and Cybernetics*, Vol. 24, no. 8, pp. 1239-1246, 1994.

Maurel, W. (1998), "3D Modeling of the Human Upper Limb including the Biomechanics of Joints, Muscles and Soft Tissues", Ph.D. Thesis, Laboratoire d'Infographie - Ecole Polytechnique Federale de Lausanne.

Morasso P, 1981, “Spatial control of arm movements”, *Exp Brain Res*, 42(2): 223-7.
Pieper, D.L. (1968), "The Kinematics of Manipulators Under Computer Control", Stanford Artificial Intelligence Laboratory, Stanford University.
Raikova, R. (1992), "A General Approach for Modelling and Mathematical Investigation of the Human Upper Limb", *Journal of Biomechanic*s, 25, 857–867.
Wood, J. E., Meek, S. G., Jacobsen, S. C., “Quantitation of human shoulder anatomy for prosthetic arm control-II. Anatomy Matrices,” *J. of Biomechanics* Vol. 22, no. 4, pp309-325, 1989.

9. Appendix A

$\mathbf{a}_1 = \{q_4 = \frac{2\pi}{3}, q_5 = 0, q_7 = 0, q_8 = 0\}$, $\mathbf{a}_2 = \{q_4 = -\frac{11\pi}{18}, q_5 = 0, q_7 = 0, q_8 = 0\}$,

$\mathbf{a}_3 = \{q_3 = -\frac{\pi}{2}, q_4 = -\frac{11\pi}{18}, q_5 = -\frac{\pi}{2}, q_8 = 0\}$, $\mathbf{a}_4 = \{q_3 = -\frac{11\pi}{18}, q_5 = \frac{\pi}{2}, q_7 = 0, q_8 = 0\}$,

$\mathbf{a}_5 = \{q_3 = \frac{\pi}{2}, q_5 = -\frac{\pi}{2}, q_7 = 0, q_8 = 0\}$, $\mathbf{a}_6 = \{q_3 = \frac{\pi}{2}, q_5 = \frac{\pi}{2}, q_7 = 0, q_8 = 0\}$,

$\mathbf{a}_7 = \{q_4 = -\frac{\pi}{2}, q_5 = -\frac{\pi}{2}, q_7 = 0, q_8 = 0\}$, $\mathbf{a}_8 = \{q_4 = \frac{\pi}{2}, q_5 = -\frac{\pi}{2}, q_7 = 0, q_8 = 0\}$,

$\mathbf{a}_9 = \{q_4 = -\frac{\pi}{2}, q_5 = \frac{\pi}{2}, q_7 = 0, q_8 = 0\}$, $\mathbf{a}_{10} = \{q_4 = \frac{\pi}{2}, q_5 = \frac{\pi}{2}, q_7 = 0, q_8 = 0\}$,

$\mathbf{a}_{11} = \{q_4 = -\frac{\pi}{2}, q_6 = 0, q_7 = 0, q_8 = 0\}$, $\mathbf{a}_{12} = \{q_4 = \frac{\pi}{2}, q_6 = 0, q_7 = 0, q_8 = 0\}$,

$\mathbf{a}_{13} = \{q_4 = -\frac{\pi}{2}, q_6 = 0, q_7 = -\frac{\pi}{3}, q_8 = 0\}$, $\mathbf{a}_{14} = \{q_4 = \frac{\pi}{2}, q_6 = 0, q_7 = -\frac{\pi}{3}, q_8 = 0\}$,

$\mathbf{a}_{15} = \{q_5 = 0, q_6 = 0, q_7 = -\frac{\pi}{3}, q_8 = 0\}$, $\mathbf{a}_{16} = \{q_4 = -\frac{\pi}{2}, q_6 = 0, q_7 = \frac{\pi}{3}, q_8 = 0\}$,

$\mathbf{a}_{17} = \{q_4 = \frac{\pi}{2}, q_6 = 0, q_7 = \frac{\pi}{3}, q_8 = 0\}$, $\mathbf{a}_{18} = \{q_5 = 0, q_6 = 0, q_7 = \frac{\pi}{3}, q_8 = 0\}$,

$\mathbf{b}_1 = \{q_3 = -\frac{\pi}{2}, q_4 = -\frac{11\pi}{18}, q_7 = 0, q_8 = 0\}$, $\mathbf{b}_2 = \{q_3 = -\frac{\pi}{2}, q_4 = \frac{2\pi}{3}, q_7 = 0, q_8 = 0\}$,

$\mathbf{b}_3 = \{q_3 = \frac{\pi}{2}, q_4 = -\frac{11\pi}{18}, q_7 = 0, q_8 = 0\}$, $\mathbf{b}_4 = \{q_3 = \frac{\pi}{2}, q_4 = \frac{2\pi}{3}, q_7 = 0, q_8 = 0\}$,

$\mathbf{b}_5 = \{q_3 = -\frac{\pi}{2}, q_5 = -\frac{\pi}{2}, q_7 = 0, q_8 = 0\}$, $\mathbf{b}_6 = \{q_3 = -\frac{\pi}{2}, q_5 = -\frac{\pi}{2}, q_6 = 0, q_8 = 0\}$,

$\mathbf{b}_7 = \{q_3 = \frac{\pi}{2}, q_5 = -\frac{\pi}{2}, q_7 = 0, q_8 = 0\}$, $\mathbf{b}_8 = \{q_3 = -\frac{\pi}{2}, q_5 = -\frac{\pi}{2}, q_6 = 0, q_8 = 0\}$,

$\mathbf{b}_9 = \{q_3 = -\frac{\pi}{2}, q_5 = \frac{\pi}{2}, q_7 = 0, q_8 = 0\}$, $\mathbf{b}_{10} = \{q_3 = -\frac{\pi}{2}, q_5 = \frac{\pi}{2}, q_6 = 0, q_8 = 0\}$,

$\mathbf{b}_{11} = \{q_3 = \frac{\pi}{2}, q_5 = \frac{\pi}{2}, q_7 = 0, q_8 = 0\}$, $\mathbf{b}_{12} = \{q_3 = \frac{\pi}{2}, q_5 = \frac{\pi}{2}, q_6 = 0, q_8 = 0\}$,

$\mathbf{b}_{13}=\{q_3=-\frac{\pi}{2},q_6=0,q_7=0,q_8=0\}$, $\mathbf{b}_{14}=\{q_3=-\frac{\pi}{2},q_5=-\frac{\pi}{2},q_6=0,q_7=0\}$,

$\mathbf{b}_{15}=\{q_3=-\frac{\pi}{2},q_5=\frac{\pi}{2},q_6=0,q_7=0\}$, $\mathbf{b}_{16}=\{q_3=\frac{\pi}{2},q_6=0,q_7=0,q_8=0\}$,

$\mathbf{b}_{17}=\{q_3=\frac{\pi}{2},q_5=-\frac{\pi}{2},q_6=0,q_7=0\}$, $\mathbf{b}_{18}=\{q_3=\frac{\pi}{2},q_5=\frac{\pi}{2},q_6=0,q_7=0\}$,

$\mathbf{b}_{19}=\{q_3=-\frac{\pi}{2},q_5=-\frac{\pi}{2},q_6=-\frac{5\pi}{6},q_7=0\}$, $\mathbf{b}_{20}=\{q_3=-\frac{\pi}{2},q_5=\frac{\pi}{2},q_6=-\frac{5\pi}{6},q_7=0\}$,

$\mathbf{b}_{21}=\{q_3=\frac{\pi}{2},q_5=-\frac{\pi}{2},q_6=-\frac{5\pi}{6},q_7=0\}$, $\mathbf{b}_{22}=\{q_3=\frac{\pi}{2},q_5=-\frac{\pi}{2},q_6=-\frac{5\pi}{6},q_7=0\}$,

$\mathbf{b}_{23}=\{q_3=-\frac{\pi}{2},q_6=0,q_7=-\frac{\pi}{3},q_8=0\}$, $\mathbf{b}_{24}=\{q_3=\frac{\pi}{2},q_6=0,q_7=-\frac{\pi}{3},q_8=0\}$,

$\mathbf{b}_{25}=\{q_3=-\frac{\pi}{2},q_6=0,q_7=\frac{\pi}{3},q_8=0\}$, $\mathbf{b}_{26}=\{q_3=\frac{\pi}{2},q_6=0,q_7=\frac{\pi}{3},q_8=0\}$,

$\mathbf{b}_{27}=\{q_4=-\frac{11\pi}{18},q_6=0,q_7=-\frac{\pi}{3},q_8=0\}$, $\mathbf{b}_{28}=\{q_4=3,q_6=0,q_7=-\frac{\pi}{3},q_8=0\}$,

$\mathbf{b}_{29}=\{q_4=-\frac{11\pi}{18},q_6=0,q_7=\frac{\pi}{3},q_8=0\}$, $\mathbf{b}_{30}=\{q_4=\frac{2\pi}{3},q_6=0,q_7=-\frac{\pi}{3},q_8=0\}$,

$\mathbf{b}_{31}=\{q_5=-\frac{\pi}{2},q_6=0,q_7=0,q_8=0\}$, $\mathbf{b}_{32}=\{q_4=-\frac{\pi}{2},q_5=-\frac{\pi}{2},q_6=0,q_7=0\}$

$\mathbf{b}_{33}=\{q_4=\frac{\pi}{2},q_5=-\frac{\pi}{2},q_6=0,q_7=0\}$, $\mathbf{b}_{34}=\{q_4=0,q_5=-\frac{\pi}{2},q_6=0,q_7=0\}$

$\mathbf{b}_{35}=\{q_5=\frac{\pi}{2},q_6=0,q_7=0,q_8=0\}$, $\mathbf{b}_{36}=\{q_4=-\frac{\pi}{2},q_5=\frac{\pi}{2},q_6=0,q_7=0\}$

$\mathbf{b}_{37}=\{q_4=\frac{\pi}{2},q_5=\frac{\pi}{2},q_6=0,q_7=0\}$, $\mathbf{b}_{38}=\{q_4=0,q_5=\frac{\pi}{2},q_6=0,q_8=0\}$

$\mathbf{b}_{39}=\{q_4=-\frac{\pi}{2},q_5=-\frac{\pi}{2},q_6=-\frac{5\pi}{6},q_7=0\}$, $\mathbf{b}_{40}=\{q_4=\frac{\pi}{2},q_5=-\frac{\pi}{2},q_6=-\frac{5\pi}{6},q_7=0\}$

$\mathbf{b}_{41}=\{q_4=-\frac{\pi}{2},q_5=\frac{\pi}{2},q_6=-\frac{5\pi}{6},q_7=0\}$, $\mathbf{b}_{42}=\{q_4=\frac{\pi}{2},q_5=\frac{\pi}{2},q_6=-\frac{5\pi}{6},q_7=0\}$

$\mathbf{b}_{43}=\{q_5=-\frac{\pi}{2},q_6=0,q_7=-\frac{\pi}{3},q_8=0\}$, $\mathbf{b}_{44}=\{q_5=\frac{\pi}{2},q_6=0,q_7=-\frac{\pi}{3},q_8=0\}$

$\mathbf{b}_{45}=\{q_5=-\frac{\pi}{2},q_6=0,q_7=\frac{\pi}{3},q_8=0\}$, $\mathbf{b}_{46}=\{q_5=\frac{\pi}{2},q_6=0,q_7=-\frac{\pi}{3},q_8=0\}$

$\mathbf{c}_1=\{q_3=-\frac{\pi}{2},q_4=-\frac{11\pi}{18},q_5=-\frac{\pi}{2},q_8=0\}$, $\mathbf{c}_2=\{q_3=\frac{\pi}{2},q_4=-\frac{11\pi}{18},q_5=-\frac{\pi}{2},q_8=0\}$

$\mathbf{c}_3=\{q_3=-\frac{\pi}{2},q_4=\frac{2\pi}{3},q_5=-\frac{\pi}{2},q_8=0\}$, $\mathbf{c}_4=\{q_3=-\frac{\pi}{2},q_4=-\frac{11\pi}{18},q_5=\frac{\pi}{2},q_8=0\}$

$\mathbf{c}_5=\{q_3=\frac{\pi}{2},q_4=\frac{2\pi}{3},q_5=-\frac{\pi}{2},q_8=0\}$, $\mathbf{c}_6=\{q_3=\frac{\pi}{2},q_4=-\frac{11\pi}{18},q_5=\frac{\pi}{2},q_8=0\}$

$$\mathbf{c}_7=\{q_3=-\frac{\pi}{2},q_4=\frac{2\pi}{3},q_5=\frac{\pi}{2},q_8=0\},\ \mathbf{c}_8=\{q_3=\frac{\pi}{2},q_4=\frac{2\pi}{3},q_5=\frac{\pi}{2},q_8=0\}$$

$$\mathbf{c}_9=\{q_3=-\frac{\pi}{2},q_4=-\frac{11\pi}{18},q_7=-\frac{\pi}{3},q_8=0\},\ \mathbf{c}_{10}=\{q_3=\frac{\pi}{2},q_4=-\frac{11\pi}{18},q_7=-\frac{\pi}{3},q_8=0\}$$

$$\mathbf{c}_{11}=\{q_3=-\frac{\pi}{2},q_4=\frac{2\pi}{3},q_7=-\frac{\pi}{3},q_8=0\},\ \mathbf{c}_{12}=\{q_3=-\frac{\pi}{2},q_4=-\frac{11\pi}{18},q_7=\frac{\pi}{3},q_8=0\}$$

$$\mathbf{c}_{13}=\{q_3=\frac{\pi}{2},q_4=\frac{2\pi}{3},q_7=-\frac{\pi}{3},q_8=0\},\ \mathbf{c}_{14}=\{q_3=\frac{\pi}{2},q_4=-\frac{11\pi}{18},q_7=\frac{\pi}{3},q_8=0\}$$

$$\mathbf{c}_{15}=\{q_3=-\frac{\pi}{2},q_4=\frac{2\pi}{3},q_7=\frac{\pi}{3},q_8=0\},\ \mathbf{c}_{16}=\{q_3=\frac{\pi}{2},q_4=\frac{2\pi}{3},q_7=\frac{\pi}{3},q_8=0\}$$

$$\mathbf{c}_{17}=\{q_3=-\frac{\pi}{2},q_4=-\frac{11\pi}{18},q_6=0,q_7=0\},\ \mathbf{c}_{18}=\{q_3=\frac{\pi}{2},q_4=-\frac{11\pi}{18},q_6=0,q_7=0\}$$

$$\mathbf{c}_{19}=\{q_3=-\frac{\pi}{2},q_4=\frac{2\pi}{3},q_6=0,q_7=0\},\ \mathbf{c}_{20}=\{q_3=-\frac{\pi}{2},q_4=-\frac{11\pi}{18},q_6=-\frac{5\pi}{6},q_7=0\}$$

$$\mathbf{c}_{21}=\{q_3=\frac{\pi}{2},q_4=\frac{2\pi}{3},q_6=0,q_7=0\},\ \mathbf{c}_{22}=\{q_3=\frac{\pi}{2},q_4=-\frac{11\pi}{18},q_6=-\frac{5\pi}{6},q_7=0\}$$

$$\mathbf{c}_{23}=\{q_3=-\frac{\pi}{2},q_4=\frac{2\pi}{3},q_6=-\frac{5\pi}{6},q_7=0\},\ \mathbf{c}_{24}=\{q_3=\frac{\pi}{2},q_4=\frac{2\pi}{3},q_6=-\frac{5\pi}{6},q_7=0\}$$

$$\mathbf{c}_{25}=\{q_3=-\frac{\pi}{2},q_4=-\frac{11\pi}{18},q_7=-\frac{\pi}{9},$$
$$q_6=-\arccos\left(\frac{2(-16+8\cos q_8+3\cos q_8^{\,2}-\sqrt{-48\sin q_8^{\,2}+104\cos q_8\sin q_8^{\,2}-35\cos q_8^{\,2}\sin q_8^{\,2}+4\sin q_8^{\,4}})}{16+8\cos q_8+\cos q_8^{\,2}+4\sin q_8^{\,2}}\right)\}$$

$$\mathbf{c}_{26}=\{q_3=-\frac{\pi}{2},q_4=-\frac{11\pi}{18},q_7=-\frac{\pi}{9},$$
$$q_6=-\arccos\left(\frac{2(-16+8\cos q_8+3\cos q_8^{\,2}+\sqrt{-48\sin q_8^{\,2}+104\cos q_8\sin q_8^{\,2}-35\cos q_8^{\,2}\sin q_8^{\,2}+4\sin q_8^{\,4}})}{16+8\cos q_8+\cos q_8^{\,2}+4\sin q_8^{\,2}}\right)\}$$

$$\mathbf{c}_{27}=\{q_3=\frac{\pi}{2},q_4=-\frac{11\pi}{18},q_7=-\frac{\pi}{9},$$
$$q_6=-\arccos\left(\frac{2(-16+8\cos q_8+3\cos q_8^{\,2}-\sqrt{-48\sin q_8^{\,2}+104\cos q_8\sin q_8^{\,2}-35\cos q_8^{\,2}\sin q_8^{\,2}+4\sin q_8^{\,4}})}{16+8\cos q_8+\cos q_8^{\,2}+4\sin q_8^{\,2}}\right)\}$$

$$\mathbf{c}_{28}=\{q_3=\frac{\pi}{2},q_4=-\frac{11\pi}{18},q_7=-\frac{\pi}{9},$$
$$q_6=-\arccos\left(\frac{2(-16+8\cos q_8+3\cos q_8^{\,2}+\sqrt{-48\sin q_8^{\,2}+104\cos q_8\sin q_8^{\,2}-35\cos q_8^{\,2}\sin q_8^{\,2}+4\sin q_8^{\,4}})}{16+8\cos q_8+\cos q_8^{\,2}+4\sin q_8^{\,2}}\right)\}$$

$$\mathbf{c}_{29}=\{q_3=-\frac{\pi}{2},q_4=\frac{2\pi}{3},q_7=-\frac{\pi}{9},$$
$$q_6=-\arccos\left(\frac{2(-16+8\cos q_8+3\cos q_8^{\,2}-\sqrt{-48\sin q_8^{\,2}+104\cos q_8\sin q_8^{\,2}-35\cos q_8^{\,2}\sin q_8^{\,2}+4\sin q_8^{\,4}})}{16+8\cos q_8+\cos q_8^{\,2}+4\sin q_8^{\,2}}\right)\}$$

$$\mathbf{c}_{30} = \{q_3 = -\frac{\pi}{2}, q_4 = \frac{2\pi}{3}, q_7 = -\frac{\pi}{9},$$
$$q_6 = -\arccos(\frac{2(-16+8\cos q_8+3\cos {q_8}^2+\sqrt{-48\sin {q_8}^2+104\cos q_8 \sin {q_8}^2-35\cos {q_8}^2 \sin {q_8}^2+4\sin {q_8}^4})}{16+8\cos q_8+\cos {q_8}^2+4\sin {q_8}^2})\}$$

$$\mathbf{c}_{31} = \{q_3 = -\frac{\pi}{2}, q_4 = -\frac{11\pi}{18}, q_7 = \frac{\pi}{9},$$
$$q_6 = -\arccos(\frac{2(-16+8\cos q_8+3\cos {q_8}^2-\sqrt{-48\sin {q_8}^2+104\cos q_8 \sin {q_8}^2-35\cos {q_8}^2 \sin {q_8}^2+4\sin {q_8}^4})}{16+8\cos q_8+\cos {q_8}^2+4\sin {q_8}^2})\}$$

$$\mathbf{c}_{32} = \{q_3 = -\frac{\pi}{2}, q_4 = -\frac{11\pi}{18}, q_7 = \frac{\pi}{9},$$
$$q_6 = -\arccos(\frac{2(-16+8\cos q_8+3\cos {q_8}^2+\sqrt{-48\sin {q_8}^2+104\cos q_8 \sin {q_8}^2-35\cos {q_8}^2 \sin {q_8}^2+4\sin {q_8}^4})}{16+8\cos q_8+\cos {q_8}^2+4\sin {q_8}^2})\}$$

$$\mathbf{c}_{33} = \{q_3 = \frac{\pi}{2}, q_4 = \frac{2\pi}{3}, q_7 = -\frac{\pi}{9},$$
$$q_6 = -\arccos(\frac{2(-16+8\cos q_8+3\cos {q_8}^2-\sqrt{-48\sin {q_8}^2+104\cos q_8 \sin {q_8}^2-35\cos {q_8}^2 \sin {q_8}^2+4\sin {q_8}^4})}{16+8\cos q_8+\cos {q_8}^2+4\sin {q_8}^2})\}$$

$$\mathbf{c}_{34} = \{q_3 = \frac{\pi}{2}, q_4 = \frac{2\pi}{3}, q_7 = -\frac{\pi}{9},$$
$$q_6 = -\arccos(\frac{2(-16+8\cos q_8+3\cos {q_8}^2+\sqrt{-48\sin {q_8}^2+104\cos q_8 \sin {q_8}^2-35\cos {q_8}^2 \sin {q_8}^2+4\sin {q_8}^4})}{16+8\cos q_8+\cos {q_8}^2+4\sin {q_8}^2})\}$$

$$\mathbf{c}_{35} = \{q_3 = \frac{\pi}{2}, q_4 = -\frac{11\pi}{18}, q_7 = \frac{\pi}{9},$$
$$q_6 = -\arccos(\frac{2(-16+8\cos q_8+3\cos {q_8}^2-\sqrt{-48\sin {q_8}^2+104\cos q_8 \sin {q_8}^2-35\cos {q_8}^2 \sin {q_8}^2+4\sin {q_8}^4})}{16+8\cos q_8+\cos {q_8}^2+4\sin {q_8}^2})\}$$

$$\mathbf{c}_{36} = \{q_3 = \frac{\pi}{2}, q_4 = -\frac{11\pi}{18}, q_7 = \frac{\pi}{9},$$
$$q_6 = -\arccos(\frac{2(-16+8\cos q_8+3\cos {q_8}^2+\sqrt{-48\sin {q_8}^2+104\cos q_8 \sin {q_8}^2-35\cos {q_8}^2 \sin {q_8}^2+4\sin {q_8}^4})}{16+8\cos q_8+\cos {q_8}^2+4\sin {q_8}^2})\}$$

$$\mathbf{c}_{37} = \{q_3 = -\frac{\pi}{2}, q_4 = \frac{2\pi}{3}, q_7 = \frac{\pi}{9},$$
$$q_6 = -\arccos(\frac{2(-16+8\cos q_8+3\cos {q_8}^2-\sqrt{-48\sin {q_8}^2+104\cos q_8 \sin {q_8}^2-35\cos {q_8}^2 \sin {q_8}^2+4\sin {q_8}^4})}{16+8\cos q_8+\cos {q_8}^2+4\sin {q_8}^2})\}$$

$$\mathbf{c}_{38} = \{q_3 = -\frac{\pi}{2}, q_4 = \frac{2\pi}{3}, q_7 = \frac{\pi}{9},$$
$$q_6 = -\arccos(\frac{2(-16+8\cos q_8+3\cos {q_8}^2+\sqrt{-48\sin {q_8}^2+104\cos q_8 \sin {q_8}^2-35\cos {q_8}^2 \sin {q_8}^2+4\sin {q_8}^4})}{16+8\cos q_8+\cos {q_8}^2+4\sin {q_8}^2})\}$$

$$\mathbf{c}_{39} = \{q_3 = \frac{\pi}{2}, q_4 = \frac{2\pi}{3}, q_7 = \frac{\pi}{9},$$
$$q_6 = -\arccos(\frac{2(-16+8\cos q_8+3\cos {q_8}^2-\sqrt{-48\sin {q_8}^2+104\cos q_8 \sin {q_8}^2-35\cos {q_8}^2 \sin {q_8}^2+4\sin {q_8}^4})}{16+8\cos q_8+\cos {q_8}^2+4\sin {q_8}^2})\}$$

$$\mathbf{c}_{40}=\{q_3=\frac{\pi}{2},q_4=\frac{2\pi}{3},q_7=\frac{\pi}{9},$$

$$q_6=-\arccos(\frac{2(-16+8\cos q_8+3\cos {q_8}^2+\sqrt{-48\sin {q_8}^2+104\cos q_8\sin {q_8}^2-35\cos {q_8}^2\sin {q_8}^2+4\sin {q_8}^4})}{16+8\cos q_8+\cos {q_8}^2+4\sin {q_8}^2})\}$$

$$\mathbf{c}_{41}=\{q_3=-\frac{\pi}{2},q_6=0,q_7=-\frac{\pi}{3},q_8=0\},\ \mathbf{c}_{42}=\{q_3=\frac{\pi}{2},q_6=0,q_7=-\frac{\pi}{3},q_8=0\}$$

$$\mathbf{c}_{43}=\{q_3=-\frac{\pi}{2},q_6=-\frac{5\pi}{6},q_7=-\frac{\pi}{3},q_8=0\},\mathbf{c}_{44}=\{q_3=-\frac{\pi}{2},q_6=0,q_7=\frac{\pi}{3},q_8=0\}$$

$$\mathbf{c}_{45}=\{q_3=\frac{\pi}{2},q_6=-\frac{5\pi}{6},q_7=-\frac{\pi}{3},q_8=0\},\ \mathbf{c}_{46}=\{q_3=\frac{\pi}{2},q_6=0,q_7=\frac{\pi}{3},q_8=0\}$$

$$\mathbf{c}_{47}=\{q_3=-\frac{\pi}{2},q_6=-\frac{5\pi}{6},q_7=\frac{\pi}{3},q_8=0\},\ \mathbf{c}_{48}=\{q_3=\frac{\pi}{2},q_6=-\frac{5\pi}{6},q_7=\frac{\pi}{3},q_8=0\}$$

$$\mathbf{c}_{49}=\{q_3=\frac{\pi}{4},q_5=-\frac{\pi}{2},q_6=0,q_7=-\frac{\pi}{3}\},\ \mathbf{c}_{50}=\{q_3=\frac{\pi}{4},q_5=\frac{\pi}{2},q_6=0,q_7=-\frac{\pi}{3}\}$$

$$\mathbf{c}_{51}=\{q_3=\frac{\pi}{4},q_5=-\frac{\pi}{2},q_6=-\frac{5\pi}{6},q_7=-\frac{\pi}{3}\},\ \mathbf{c}_{52}=\{q_3=\frac{\pi}{4},q_5=-\frac{\pi}{2},q_6=0,q_7=\frac{\pi}{3}\}$$

$$\mathbf{c}_{53}=\{q_3=\frac{\pi}{4},q_5=\frac{\pi}{2},q_6=-\frac{5\pi}{6},q_7=-\frac{\pi}{3}\},\ \mathbf{c}_{54}=\{q_3=\frac{\pi}{4},q_5=\frac{\pi}{2},q_6=0,q_7=\frac{\pi}{3}\}$$

$$\mathbf{c}_{55}=\{q_3=\frac{\pi}{4},q_5=-\frac{\pi}{2},q_6=-\frac{5\pi}{6},q_7=\frac{\pi}{3}\},\ \mathbf{c}_{56}=\{q_3=\frac{\pi}{4},q_5=\frac{\pi}{2},q_6=-\frac{5\pi}{6},q_7=\frac{\pi}{3}\}$$

$$\mathbf{c}_{57}=\{q_3=\frac{\pi}{4},q_5=-\frac{\pi}{2},q_6=0,q_8=-\frac{\pi}{9}\},\ \mathbf{c}_{58}=\{q_3=\frac{\pi}{4},q_5=\frac{\pi}{2},q_6=0,q_8=-\frac{\pi}{9}\}$$

$$\mathbf{c}_{59}=\{q_3=\frac{\pi}{4},q_5=-\frac{\pi}{2},q_6=-\frac{5\pi}{6},q_8=-\frac{\pi}{9}\},\ \mathbf{c}_{60}=\{q_3=\frac{\pi}{4},q_5=-\frac{\pi}{2},q_6=0,q_8=\frac{\pi}{9}\}$$

$$\mathbf{c}_{61}=\{q_3=\frac{\pi}{4},q_5=\frac{\pi}{2},q_6=-\frac{5\pi}{6},q_8=-\frac{\pi}{9}\},\ \mathbf{c}_{62}=\{q_3=\frac{\pi}{4},q_5=\frac{\pi}{2},q_6=0,q_8=\frac{\pi}{9}\}$$

$$\mathbf{c}_{63}=\{q_3=\frac{\pi}{4},q_5=-\frac{\pi}{2},q_6=-\frac{5\pi}{6},q_8=\frac{\pi}{9}\},\ \mathbf{c}_{64}=\{q_3=\frac{\pi}{4},q_5=\frac{\pi}{2},q_6=-\frac{5\pi}{6},q_8=\frac{\pi}{9}\}$$

$$\gamma_1=\{q_6=0,q_7=-\frac{\pi}{3},q_8=-\frac{\pi}{9}\},\ \gamma_2=\{q_6=-\frac{5\pi}{6},q_7=-\frac{\pi}{3},q_8=-\frac{\pi}{9}\}$$

$$\gamma_3=\{q_6=0,q_7=\frac{\pi}{3},q_8=-\frac{\pi}{9}\},\ \gamma_4=\{q_6=0,q_7=-\frac{\pi}{3},q_8=\frac{\pi}{9}\}$$

$$\gamma_5=\{q_6=-\frac{5\pi}{6},q_7=\frac{\pi}{3},q_8=-\frac{\pi}{9}\},\ \gamma_6=\{q_6=-\frac{5\pi}{6},q_7=-\frac{\pi}{3},q_8=\frac{\pi}{9}\}$$

$$\gamma_7=\{q_6=0,q_7=\frac{\pi}{3},q_8=\frac{\pi}{9}\},\ \gamma_8=\{q_6=-\frac{5\pi}{6},q_7=\frac{\pi}{3},q_8=\frac{\pi}{9}\}$$

$\gamma_9\ldots\gamma_{24}$ Sixteen combinations $q_3=\begin{Bmatrix}-\pi/2\\ \pi/2\end{Bmatrix}$, $q_4=\begin{Bmatrix}-11\pi/18\\ 2\pi/3\end{Bmatrix}$, $q_5=\begin{Bmatrix}-\pi/2\\ \pi/2\end{Bmatrix}$,

and $q_6=\begin{Bmatrix}-5\pi/6\\ 0\end{Bmatrix}$,

$\gamma_{25}\ldots\gamma_{40}$ Sixteen combinations $q_3=\begin{Bmatrix}-\pi/2\\ \pi/2\end{Bmatrix}$, $q_4=\begin{Bmatrix}-11\pi/18\\ 2\pi/3\end{Bmatrix}$, $q_5=\begin{Bmatrix}-\pi/2\\ \pi/2\end{Bmatrix}$, and $q_7=\begin{Bmatrix}-\pi/3\\ \pi/3\end{Bmatrix}$,

$\gamma_{41}\ldots\gamma_{56}$ Sixteen combinations $q_3=\begin{Bmatrix}-\pi/2\\ \pi/2\end{Bmatrix}$, $q_4=\begin{Bmatrix}-11\pi/18\\ 2\pi/3\end{Bmatrix}$, $q_5=\begin{Bmatrix}-\pi/2\\ \pi/2\end{Bmatrix}$, and $q_8=\begin{Bmatrix}-\pi/9\\ \pi/9\end{Bmatrix}$,

$\gamma_{57}\ldots\gamma_{72}$ Sixteen combinations $q_3=\begin{Bmatrix}-\pi/2\\ \pi/2\end{Bmatrix}$, $q_4=\begin{Bmatrix}-11\pi/18\\ 2\pi/3\end{Bmatrix}$, $q_6=\begin{Bmatrix}-5\pi/6\\ 0\end{Bmatrix}$, $q_7=\begin{Bmatrix}-\pi/3\\ \pi/3\end{Bmatrix}$,

$\gamma_{73}\ldots\gamma_{88}$ Sixteen combinations $q_3=\begin{Bmatrix}-\pi/2\\ \pi/2\end{Bmatrix}$, $q_4=\begin{Bmatrix}-11\pi/18\\ 2\pi/3\end{Bmatrix}$, $q_6=\begin{Bmatrix}-5\pi/6\\ 0\end{Bmatrix}$, $q_8=\begin{Bmatrix}-\pi/9\\ \pi/9\end{Bmatrix}$,

$\gamma_{89}\ldots\gamma_{104}$ Sixteen combinations $q_3=\begin{Bmatrix}-\pi/2\\ \pi/2\end{Bmatrix}$, $q_4=\begin{Bmatrix}-11\pi/18\\ 2\pi/3\end{Bmatrix}$, $q_7=\begin{Bmatrix}-\pi/3\\ \pi/3\end{Bmatrix}$, $q_8=\begin{Bmatrix}-\pi/9\\ \pi/9\end{Bmatrix}$,

$\gamma_{105}\ldots\gamma_{120}$ Sixteen combinations $q_3=\begin{Bmatrix}-\pi/2\\ \pi/2\end{Bmatrix}$, $q_5=\begin{Bmatrix}-\pi/2\\ \pi/2\end{Bmatrix}$, $q_6=\begin{Bmatrix}-5\pi/6\\ 0\end{Bmatrix}$, $q_7=\begin{Bmatrix}-\pi/3\\ \pi/3\end{Bmatrix}$,

$\gamma_{121}\ldots\gamma_{136}$ Sixteen combinations $q_3=\begin{Bmatrix}-\pi/2\\ \pi/2\end{Bmatrix}$, $q_5=\begin{Bmatrix}-\pi/2\\ \pi/2\end{Bmatrix}$, $q_6=\begin{Bmatrix}-5\pi/6\\ 0\end{Bmatrix}$, $q_8=\begin{Bmatrix}-\pi/9\\ \pi/9\end{Bmatrix}$,

$\gamma_{137}\ldots\gamma_{152}$ Sixteen combinations $q_3=\begin{Bmatrix}-\pi/2\\ \pi/2\end{Bmatrix}$, $q_5=\begin{Bmatrix}-\pi/2\\ \pi/2\end{Bmatrix}$, $q_7=\begin{Bmatrix}-\pi/3\\ \pi/3\end{Bmatrix}$, $q_8=\begin{Bmatrix}-\pi/9\\ \pi/9\end{Bmatrix}$,

$\gamma_{153}\ldots\gamma_{168}$ Sixteen combinations $q_4=\begin{Bmatrix}-11\pi/18\\ 2\pi/3\end{Bmatrix}$, $q_5=\begin{Bmatrix}-\pi/2\\ \pi/2\end{Bmatrix}$, $q_6=\begin{Bmatrix}-5\pi/6\\ 0\end{Bmatrix}$, $q_7=\begin{Bmatrix}-\pi/3\\ \pi/3\end{Bmatrix}$,

$\gamma_{169}\ldots\gamma_{184}$ Sixteen combinations $q_4=\begin{Bmatrix}-11\pi/18\\ 2\pi/3\end{Bmatrix}$, $q_5=\begin{Bmatrix}-\pi/2\\ \pi/2\end{Bmatrix}$, $q_6=\begin{Bmatrix}-5\pi/6\\ 0\end{Bmatrix}$,
$q_8=\begin{Bmatrix}-\pi/9\\ \pi/9\end{Bmatrix}$,

$\gamma_{185}\ldots\gamma_{200}$ Sixteen combinations $q_4=\begin{Bmatrix}-11\pi/18\\ 2\pi/3\end{Bmatrix}$, $q_5=\begin{Bmatrix}-\pi/2\\ \pi/2\end{Bmatrix}$, $q_7=\begin{Bmatrix}-\pi/3\\ \pi/3\end{Bmatrix}$,
$q_8=\begin{Bmatrix}-\pi/9\\ \pi/9\end{Bmatrix}$,

$\gamma_{201}\ldots\gamma_{216}$ Sixteen combinations $q_3=\begin{Bmatrix}-\pi/2\\ \pi/2\end{Bmatrix}$, $q_6=\begin{Bmatrix}-5\pi/6\\ 0\end{Bmatrix}$, $q_7=\begin{Bmatrix}-\pi/3\\ \pi/3\end{Bmatrix}$,
$q_8=\begin{Bmatrix}-\pi/9\\ \pi/9\end{Bmatrix}$,

$\gamma_{217}\ldots\gamma_{232}$ Sixteen combinations $q_4=\begin{Bmatrix}-11\pi/18\\ 2\pi/3\end{Bmatrix}$, $q_6=\begin{Bmatrix}-5\pi/6\\ 0\end{Bmatrix}$, $q_7=\begin{Bmatrix}-\pi/3\\ \pi/3\end{Bmatrix}$,
$q_8=\begin{Bmatrix}-\pi/9\\ \pi/9\end{Bmatrix}$.